

Journal Pre-proof

Proteomic profiling reveals mitochondrial alterations in Rett syndrome

Vittoria Cicaloni, Alessandra Pecorelli, Laura Tinti, Marco Rossi, Mascia Benedusi, Carlo Cervellati, Ottavia Spiga, Annalisa Santucci, Joussef Hayek, Laura Salvini, Cristina Tinti, Giuseppe Valacchi



PII: S0891-5849(20)30857-1

DOI: <https://doi.org/10.1016/j.freeradbiomed.2020.05.014>

Reference: FRB 14703

To appear in: *Free Radical Biology and Medicine*

Received Date: 24 April 2020

Revised Date: 14 May 2020

Accepted Date: 16 May 2020

Please cite this article as: V. Cicaloni, A. Pecorelli, L. Tinti, M. Rossi, M. Benedusi, C. Cervellati, O. Spiga, A. Santucci, J. Hayek, L. Salvini, C. Tinti, G. Valacchi, Proteomic profiling reveals mitochondrial alterations in Rett syndrome, *Free Radical Biology and Medicine* (2020), doi: <https://doi.org/10.1016/j.freeradbiomed.2020.05.014>.

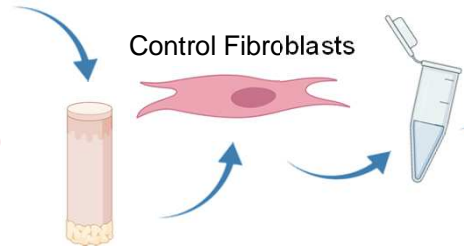
This is a PDF file of an article that has undergone enhancements after acceptance, such as the addition of a cover page and metadata, and formatting for readability, but it is not yet the definitive version of record. This version will undergo additional copyediting, typesetting and review before it is published in its final form, but we are providing this version to give early visibility of the article. Please note that, during the production process, errors may be discovered which could affect the content, and all legal disclaimers that apply to the journal pertain.

© 2020 Published by Elsevier Inc.

Control Subjects



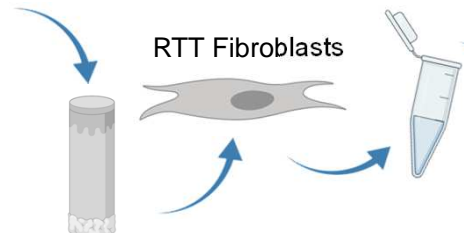
Control Fibroblasts



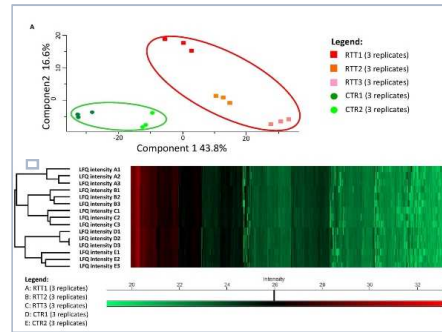
RTT Patients



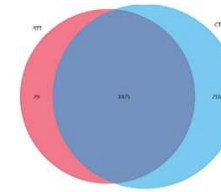
RTT Fibroblasts



MS analysis



Data analysis



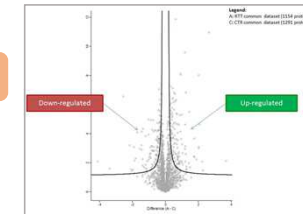
↑ Cellular Component

- Mitochondrion

↓ Biological Processes:

- Cell Growth and/or Maintenance
- Energy Pathway
- Protein Metabolism
- Mitochondrion Organization and Biogenesis

Bioinformatics



↑ DEPs:

- ATP5MG
- COX6B1
- CYB5R3
- PRDX5

Validation

Altered gene expression:

- Mitochondrial Fusion Components
- Mitophagy Component

Impaired Mitophagy Pathway

Abnormal Mitochondrial Morphology



Proteomic profiling reveals mitochondrial alterations in Rett Syndrome

Vittoria Cicaloni¹, Alessandra Pecorelli², Laura Tinti¹, Marco Rossi¹, Mascia Benedusi³, Carlo Cervellati⁴, Ottavia Spiga⁵, Annalisa Santucci⁵, Joussef Hayek⁶, Laura Salvini¹, Cristina Tinti¹, Giuseppe Valacchi^{2,3,7*}.

¹Toscana Life Science Foundation, Via Fiorentina 1, 53100 Siena, Italy;

²Plants for Human Health Institute, Animal Science Dept., NC Research Campus, NC State University, 600 Laureate Way, Kannapolis, NC 28081, USA;

³Department of Biomedical and Specialist Surgical Sciences, Section of Medical Biochemistry, Molecular Biology and Genetics, University of Ferrara, Ferrara, Italy;

⁴Department of Morphology and Experimental Medicine University of Ferrara via Borsari 46, 44121 Ferrara (Italy)

⁵Department of Biotechnology, Chemistry and Pharmacy, Via Aldo Moro 2, University of Siena, Siena, Italy;

⁶Child Neuropsychiatry Unit, University General Hospital, Azienda Ospedaliera Universitaria Senese, Viale M. Bracci 16, 53100 Siena, Italy;

⁷Kyung Hee University, Department of Food and Nutrition, Seoul, South Korea.

*Corresponding Author

Prof. Giuseppe Valacchi

gvalacc@ncsu.edu

600 Laureate Way, Kannapolis, NC USA

PHHI, Department of Animal Science

Abstract

Rett syndrome (RTT) is a pervasive neurodevelopmental disorder associated with mutation in *MECP2* gene. Despite a well-defined genetic cause, there is a growing consensus that a metabolic component could play a pivotal role in RTT pathophysiology. Indeed, perturbed redox homeostasis and inflammation, i.e. oxinflammation, with mitochondria dysfunction as the central hub between the two phenomena, appear as possible key contributing factors to RTT pathogenesis and its clinical features. While these RTT-related changes have been widely documented by transcriptomic profiling, proteomics studies supporting these evidences are still limited.

Here, using primary dermal fibroblasts from control and patients, we perform a large-scale proteomic analysis that, together with data mining approaches, allow us to carry out the first comprehensive characterization of RTT cellular proteome, showing mainly changes in expression of proteins involved in the mitochondrial network. These findings parallel with an altered expression of key mediators of mitochondrial dynamics and mitophagy associated with abnormal mitochondrial morphology. In conclusion, our proteomic analysis confirms the pathological relevance of mitochondrial dysfunction in RTT pathogenesis and progression.

Keywords: MeCP2, mitofusins, volcano plot, mitochondrial dynamic, mitophagy

Introduction

Mutations in the gene encoding the intrinsically disordered protein methyl-CpG-binding-domain-containing-protein 2 (*MECP2*) are the main cause of typical Rett syndrome (RTT; OMIN #312750), a devastating neurodevelopmental disorder that affects mostly females with an estimated incidence of one in 10,000-15,000 live births [1]. In the typical form, affected individuals display an apparently normal psychomotor development for the first 6-18 months of life. Subsequently, after a short stagnation stage, a characteristic regression occurs with loss of hand skills, spoken language and appearance of autism-like behaviors [2]. In addition to the neurological symptoms, other progressive multisystem complications include gastrointestinal issues, irregular breathing patterns, epilepsy, cardiac irregularities and Parkinson's-like motor deficits [3].

Despite the known genetic cause of RTT and almost two decades of research into the MeCP2 functions, little is known about the molecular mechanisms leading from its mutation to the disease development and progression [4]. In addition, a metabolic component appears to contribute to the phenotypical manifestations of RTT [5]. In recent years, a harmful crosstalk between an aberrant immune response and an altered redox homeostasis, so-called oxinflammation phenomenon, has been implicated as a potentially key player in RTT [6–8]. Evidence of a subclinical inflammation arises from an unusual high production of cytokines and perturbed cell immune function [7,9]. While the imbalance toward a pro-oxidative state is associated with a defective enzymatic antioxidant defense coupled to an increased production of reactive oxygen species (ROS) [6,10].

Multiple elements support the idea that mitochondria could play a role as the central hub in RTT oxinflammation [6,7,10–15]. RTT shares common clinical aspects with mitochondrial disorders including developmental delay, muscle weakness, dystonia, movement disorders, spasms, tremors, cardio-respiratory disturbances, and seizures [11,12]. Similarly, to the defined mitochondriopathies, RTT is also characterized by atypical mitochondrial morphology and bioenergetics with decreased ATP production and aberrant oxidant generation [10–13,15–17]. Moreover, dysfunctional mitochondria and altered redox homeostasis appear as a common denominators for RTT and other neurodevelopment diseases such as Down syndrome, Fragile X syndrome and autism [15,18].

In a previous microarray study on mRNA isolated from human peripheral blood lymphomonocytes (PBMC), our group found an altered gene expression profile in RTT, mainly characterized by the overexpression of transcripts related to mitochondrial organization and function; probably a cellular compensatory mechanism adopted to cope with an increased energy demand for the degradation of damaged proteins [16]. In fact, in addition to mitochondrial-related genes, also transcripts linked to ubiquitin-proteasome pathways and antioxidant defense showed an upregulated expression [16]. All

together, these findings prompted us to further investigate mitochondria in RTT. Using a proteomic data mining approach, we first directed our investigation on the protein expression signatures of primary dermal fibroblasts obtained from RTT patients and healthy controls, a very reliable model to study this syndrome [19], focusing mainly on the proteins related to mitochondrial network. In other studies, alterations of mitochondrial proteome have been associated with the disruption of dynamic processes such as biogenesis, fusion-fission cycles and mitophagy that, operating in a coordinate way, are responsible to preserve mitochondrial function by regulating their morphology, size and number [20–23]. Impaired mitochondrial dynamics and quality control processes are associated with the development and progression of different pathologies including neurological and neurodevelopmental disorders, cardiovascular and metabolic diseases [15,20–23]. In previous reports, a decreased expression of peroxisome proliferator-activated receptor gamma coactivator 1-alpha (PGC-1 α), a transcription factor that controls mitochondrial biogenesis and fusion, was observed in human primary RTT fibroblasts and skeletal muscle of symptomatic *Mecp2*-null mice [10,24]. Moreover, abnormal mitochondrial morphology and ultrastructure have been reported in RTT [11,12,15,17]. However, except for this evidence, other processes related to mitochondrial dynamics and quality control remain largely unexplored in RTT, although a role for these pathways has already been highlighted in other neurodevelopmental disorders, including autism, and potentially suggested for RTT [15,18].

In this study, using an *ex-vivo* model, i.e. primary dermal fibroblasts, and a proteomic data mining approach, we have been able to clearly confirm the involvement of mitochondrial dysfunction in RTT. From the large amounts of data generated by our large-scale proteomic analysis, using data mining and bioinformatics methods, we uncovered a proteome profile indicative of mitochondrial dysfunction in RTT. Moreover, aberrant mitochondrial dynamics and mitophagy associated with defects in mitochondrial morphology further corroborated our proteomic findings.

Results

Proteomics analysis

In a previous study by Pecorelli et al. [16], a microarray-based transcriptome-profiling revealed almost 500 differentially expressed genes in RTT PBMC, mainly upregulated transcripts related to key biological pathways such as mitochondrial function/organization and ubiquitination/proteasome system. While other transcriptomic investigations on RTT biological samples corroborated the microarray results, in particular regarding the atypical expression of mitochondrial-related genes [25], proteomics analyses are still quite limited in RTT [26–30]. Moreover, it is worth mentioning that a change in gene expression is not always associated with similar patterns in protein abundance. In this regard, the study of the proteomic consequences of *MECP2* mutation could provide a better understanding of the underlying complex pathological processes of RTT. Considering this, we decided to conduct a first qualitative proteomics analysis on primary dermal fibroblasts obtained from control (CTR) and RTT subjects. Primary cultures of skin fibroblasts represent a valid cell model for studying RTT and other neurological disorders [19]. Further filtering was applied in proteins selection for three RTT cell lines:

- RTT1 (three replicates with a total amount of proteins equal to 2046, 2016 and 1915 respectively),
- RTT2 (three replicates: 2007, 1927 and 1924 proteins respectively),
- RTT3 (three replicates: 1541, 1463 and 1418 proteins respectively).

For CTR cell lines, we have considered two samples:

- CTR1 (three replicates: 2049, 2051 and 2071 proteins respectively),
- CTR2 (three replicates: 1542, 1690 and 1690 proteins respectively).

A quality control filtering of mass spectrometry measurements was performed and showed in Supplementary Material S1. For RTT, 1154 quantifiable unique proteins with association to a known *Homo sapiens* gene were found in common in the three samples; whereas for CTR the common dataset is represented by 1291. A numeric comparison between the common RTT subset (1154 proteins) and CTR subset (1291 proteins) was performed and showed in a Venn diagram (Fig. 1).

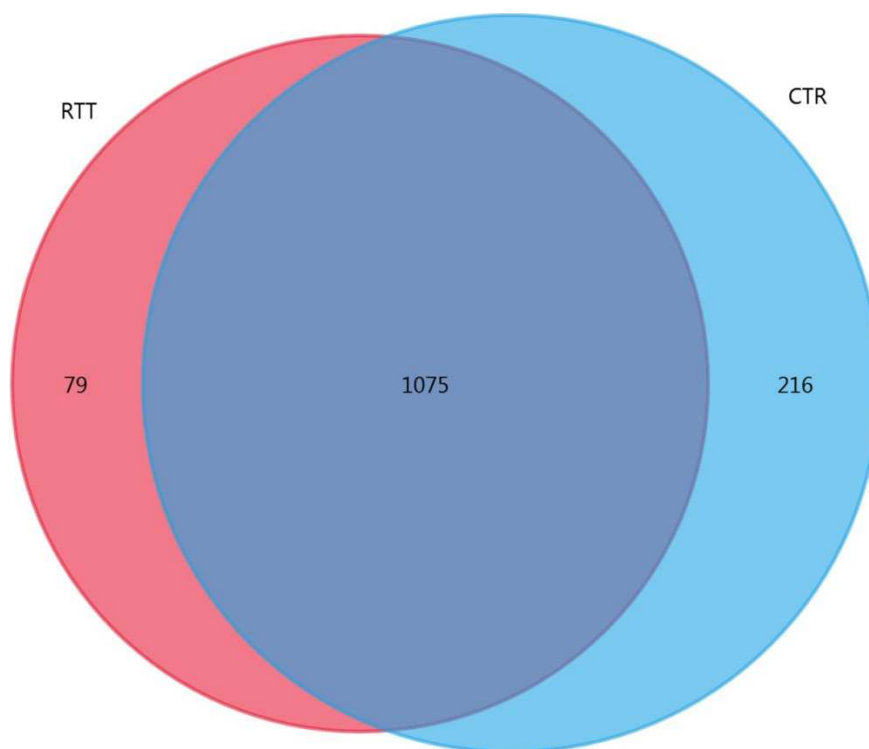


Fig 1. Preliminary proteomics analysis. Venn diagram representing the number of reproducibly quantified proteins for CTR (1291 total proteins) and RTT (1154 total proteins) fibroblasts.

For comparisons across the two distinct cell types, the resultant average “overlap index” was calculated and Jaccard similarity coefficient (which measures similarity between finite sample sets and it is defined as the size of the intersection divided by the size of the union of the sample sets) resulted to be 0.78. For CTR, the 16.73% of the total proteome is unique while the 83.27% is in common with RTT. Similarly, for RTT sample the 6.85% of the whole protein dataset is unique while 93.15% was in common with CTR. In order to mine useful information in comparing RTT and CTR, such proteomics datasets have been further classified and investigated. Clustering methods, such as hierarchical clustering, are often used for finding expression patterns of groups of proteins and for their visualization in a heat map where columns indicate the samples and rows indicate the proteins (Fig. 2B) [31]. To find statistically significant changes between RTT and CTR, hierarchical clustering of the raw intensities was performed by using Euclidean distances among label-free quantification (LFQ) intensities. Clustering tree resulting from unsupervised clustering of samples showed a clearer differentiation between RTT and CTR (Fig. 2B).

Principal Component Analysis (PCA) is an alternative method of visualizing the main clusters in the data and the relatedness between samples [31]. In order to explore the sample separation and cluster, we have performed a PCA where the first two principal components explained 60.4% of the variation, confirming an acceptably large percentage. All the triplicates of CTR and RTT samples

included in the analysis appeared to cluster in two distinct groups, confirming a clear proteomic differentiation between CTR and RTT dataset (Fig. 2A).

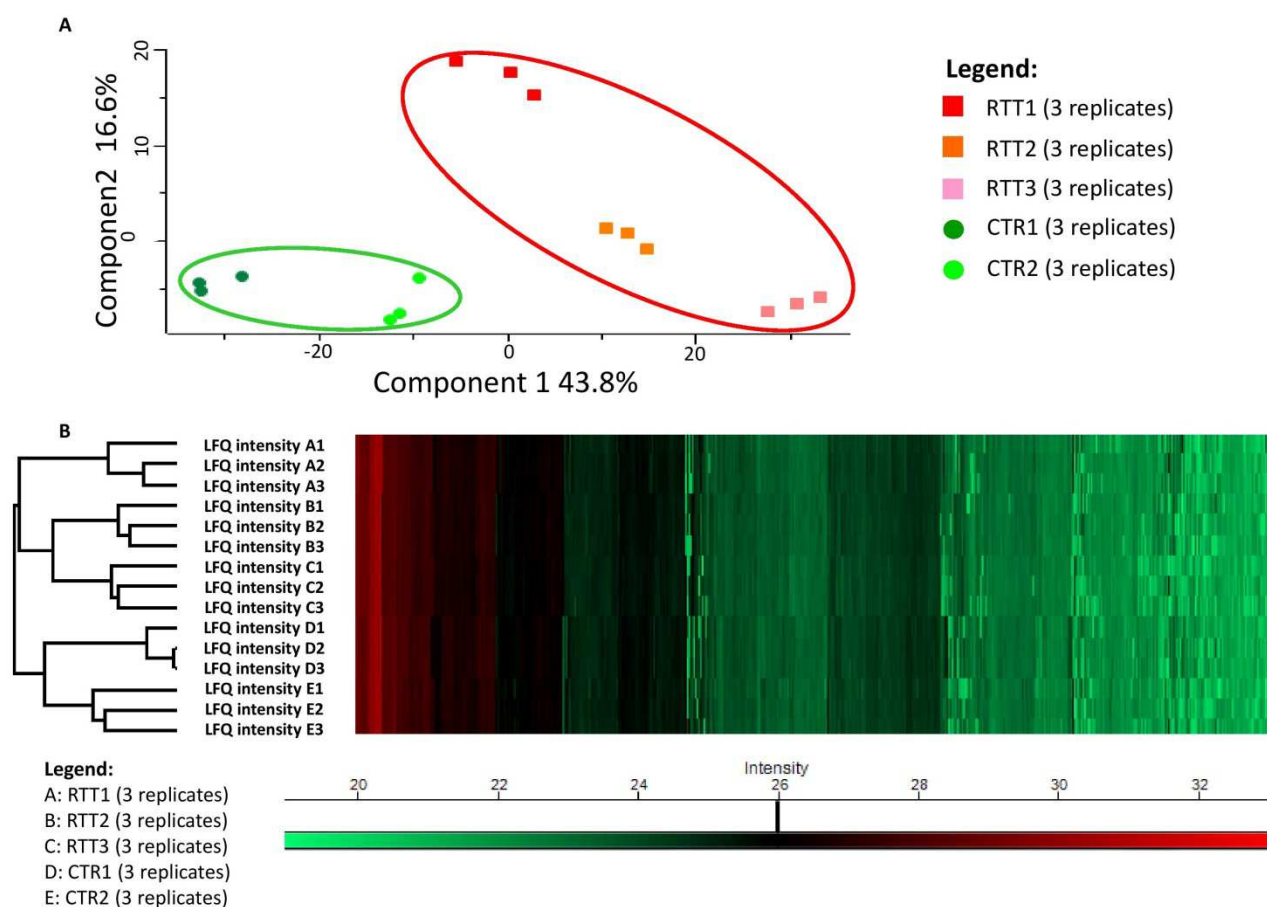


Fig 2. Preliminary analysis. **A)** PCA-biplot showing a principal component analysis of all CTR and RTT samples analyzed by mass spectrometry. The percentage of the variance contributed by each principal component is indicated in the axis: 43.8% for the first component and 16.6% for the second component. **B)** Hierarchical clustering. Heatmap shows LFQ intensity values for triplicates of every sample (A, B and C are triplicates of RTT samples and C, D are triplicates of CTR samples). Within each group, proteins are sorted in according to their LFQ intensity values: red (max value), green (min value). Clustering tree resulting from unsupervised clustering of samples is shown on top and confirms a differentiation between RTT and CTR samples.

A statistically significant (p -value < 0.001) difference between RTT and CTR subsets was also detectable in terms of GO annotations related to basal biological processes like cell growth and/or maintenance (GO:0016049), energy pathway (GO:0006091) and protein metabolism (GO:0051246). This is a preliminary observation to indicate that the percentage of proteins involved in previous cited GOs are lower in RTT than in CTR (see supplementary materials S2). In particular, the percentage of proteins involved in the process in which a cell irreversibly increases in size over time by accretion and biosynthetic production of matter [32] is higher in CTR, indicating a deficiency in RTT samples in the number of proteins involved in cell growth and/or maintenance (GO:0016049). The same is true for the process concerning chemical reactions and pathways

resulting in the formation of precursor metabolites, substances from which energy is derived, and any process involved in the liberation of energy from these substances and for the process that modulates the frequency, rate or extent of the chemical reactions and pathways involving protein metabolism (GO:0006091) [32]. Summarizing, such evidences could be linked to a general decrease in the number of proteins implicated in the principal functions of RTT cells in comparison to CTR. On the contrary, the percentage of proteins involved in the cellular component mitochondrion (GO:0005739) resulted to be higher in RTT rather than in CTR common dataset (p-value < 0.001) (see supplementary materials S2). However, the GO term related to “mitochondrial organization and biogenesis” (GO:0007005) resulted under-represented in RTT cell lines in comparison to CTR cell lines (p-value < 0.01). Proteins linked to this biological process participate in mitochondrial formation, assembly, or disassembly (for example mitochondrial fusion and fission processes). In addition, this classification also includes proteins associated with mitochondrial morphology and distribution, replication of mitochondrial genome, and synthesis of new mitochondrial constituents. In eukaryotic cells, mitochondria are the primary organelles involved in energy production. Consequently, changes in mitochondrial protein expression patterns could impair their metabolic activity in generating ATP. In this context, our proteomics data support previous studies demonstrating mitochondrial bioenergetics impairment in RTT [10–12]. Furthermore, these findings are also consistent with previous transcriptomic analyses showing a direct or indirect involvement of MeCP2 in regulating the expression of several nuclear genes encoding mitochondrial factors [16,33,34]. Based on these findings, we decided to focus this study on the up/down regulated proteins and specifically we have selected those included in mitochondrion. In Fig. 3, it is possible to notice the Volcano plot of RTT common dataset in comparison to CTR common dataset; we have found a total of 244 statistically significant proteins with up/down regulation.

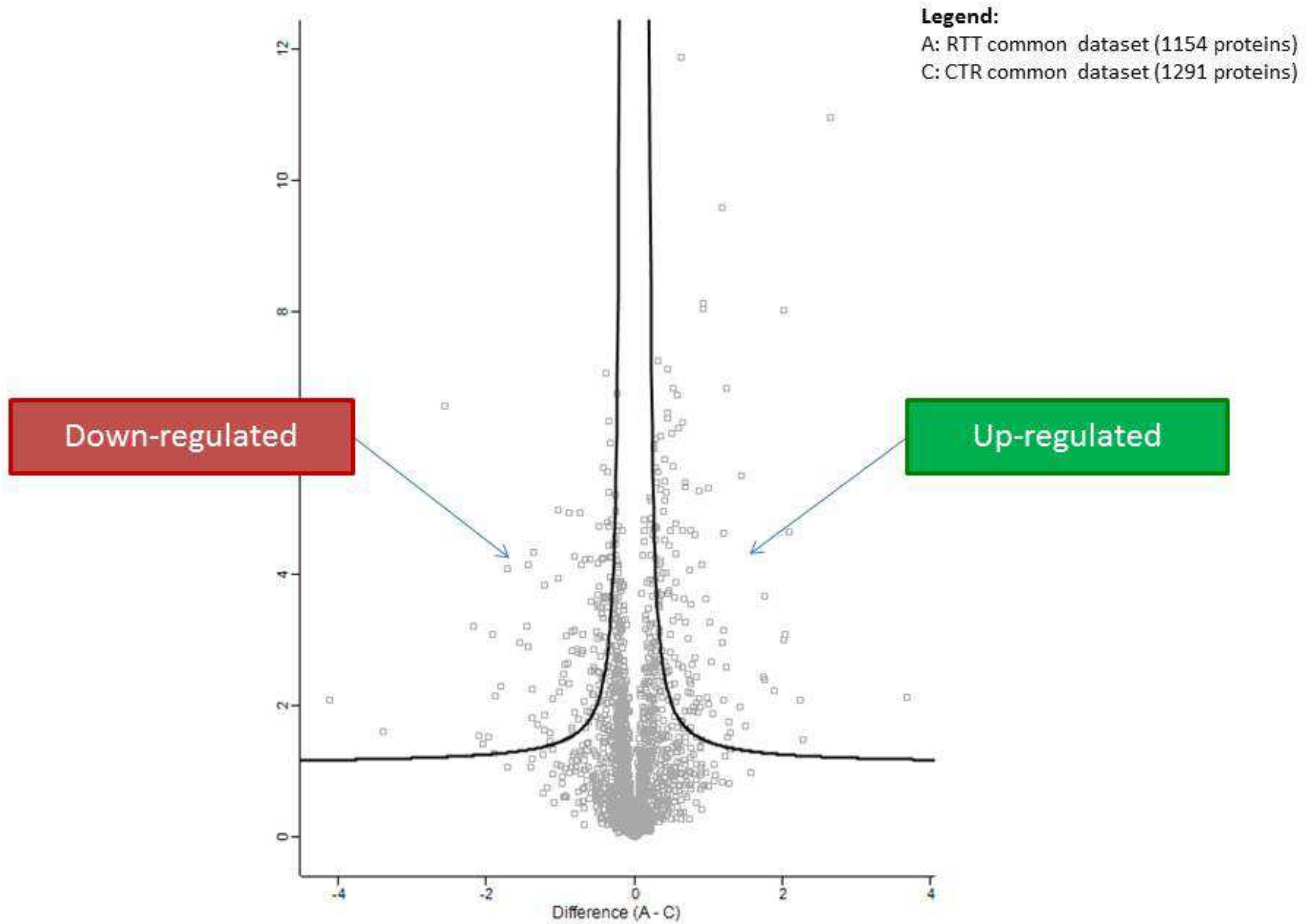


Fig. 3. Volcano plot. Volcano plot showing proteins differentially expressed between two RTT and CTR datasets. Proteins with statistically significant differential expression (difference (A) RTT– (C) CTR $\geq \pm 1.5$, FDR < 0.05) located in the top right and left quadrants.

A subset of the proteins differentially expressed in RTT in comparison to CTR belonged to mitochondrion cellular component (p-value < 0.001). In particular, such proteins showed up-regulated levels in RTT fibroblasts (Table 1).

Table 1. Mitochondrial proteins extrapolated by volcano plot and resulted to be up-regulated in RTT fibroblasts.

FDR	UniProt Accession	UniProt ID/Name	Gene	Up/down in RTT
< 0.05	O75964	ATP5L_HUMAN ATP synthase subunit g, mitochondrial	ATP5MG	Up
< 0.05	P14854	CX6B1_HUMAN Cytochrome c oxidase subunit 6B1	COX6B1	Up
< 0.05	P00387	NB5R3_HUMAN NADH-cytochrome b5 reductase 3	CYB5R3	Up
< 0.05	P30044	PRDX5_HUMAN Peroxiredoxin-5,mitochondrial	PRDX5	Up

- “ATP synthase subunit g, mitochondrial” (UniProt accession: P00387) is a subunit of the F₀ domain in ATP synthase, also known as complex V. This large protein complex, composed of 16 different subunits organized in two functional domains F₀ and F₁, utilizes the electrochemical gradient of protons generated by the respiratory chain complexes across the inner mitochondrial membrane to produce ATP from ADP. Moreover, ATP synthase dimerization and oligomerization play a critical role in regulating mitochondrial cristae architecture [35].
- “Cytochrome c oxidase 6B1” (Uniprot accession: P14854) is a subunit of the cytochrome c oxidase (GO:0004129), also known as complex IV, the last enzyme in the mitochondrial electron transport chain. In particular, this multisubunit enzyme composed of 14 subunits catalyzes the reduction of oxygen to water accompanied by the extrusion of four protons from the mitochondrial matrix to the intermembrane space, forming a proton gradient utilized by ATP synthase for the synthesis of ATP [36].
- “NADH-cytochrome b5 reductase 3” (Uniprot accession: P00387) is a flavoprotein reductase that mediates electron transfer from the electron donor NADH to the acceptor cytochrome b5. Its membrane-bound isoform, attached to the mitochondrial outer membrane, endoplasmic reticulum, and plasma membrane, is involved in elongation and unsaturation of fatty acids, cholesterol biosynthesis, and drug metabolism. Furthermore, this enzyme contributes to the protection against lipid peroxidation by maintaining molecules such as coenzyme Q, α -tocopherol, and ascorbate in their reduced form. By the maintenance of an optimal NAD⁺/NADH ratio, NADH-cytochrome b5 reductase 3 plays an essential role in the regulation of metabolic homeostasis linked to mitochondrial respiration rate, ATP production, and mitochondrial electron transport chain activity [37].
- “Peroxiredoxin-5, mitochondrial” (Uniprot accession: P30044), a member of the peroxiredoxin family, is a thiol-specific peroxidase that catalyzes the reduction of hydrogen peroxide (H₂O₂) and organic hydroperoxides to water and alcohols, respectively. It plays a role in cell protection against oxidative stress by detoxifying peroxides and as sensor of H₂O₂-mediated signaling events [38].

As it is well known, MeCP2 is a global regulator of transcription [5]. Therefore, to understand if the differentially expressed proteins identified in our proteomics study depended on a dysregulated expression of the corresponding genes, due to the absence of a functional MeCP2, or rather from other post-transcriptional regulatory mechanisms, we performed a quantitative real-time PCR for COX6B1, CYB5R3, and PRDX5. As shown in Fig. 4, consistent with our proteomic data, gene expression levels of COX6B1, CYB5R3, and PRDX5 were significantly upregulated in RTT in

comparison to CTR fibroblasts, showing a strong relationship between protein levels and their coding transcripts.

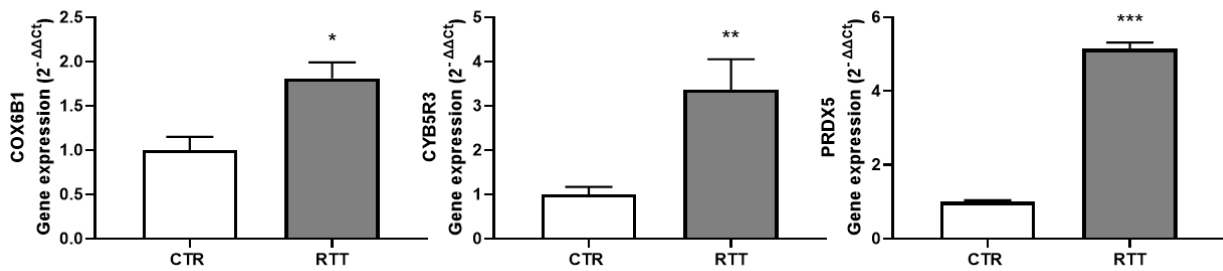


Figure 4. Quantitative real-time polymerase chain reaction (qRT-PCR) of the transcript levels for three proteins differentially expressed in RTT in comparison to CTR. The gene expression levels of COX6B1, CYB5R3 and PRDX5 were upregulated in RTT fibroblasts in comparison to CTR. The average of CTR samples was set as 1. For each gene, expression levels were normalized to GAPDH using the delta Ct method. Data are represented as mean \pm SEM. p values in relation to CTR were calculated using a Student's t test and set to the following scale: * $p < 0.05$; ** $p < 0.01$; *** $p < 0.001$.

Altered expression of key components of mitochondrial fusion machinery and mitophagy in RTT cells

Among the differentially expressed proteins, ATP synthase subunit g, mitochondrial and cytochrome c oxidase 6B1 (i.e. ATP5MG and COX6B1) are clearly linked to the mitochondrial bioenergetic function and cristae structure, while NADH-cytochrome b5 reductase 3 and mitochondrial peroxiredoxin-5 (i.e. CYB5R3 and PRDX5) are implicated in the maintenance of cellular redox balance. Interestingly, in other proteomics studies, alterations in the expression of proteins involved in mitochondrial energy metabolism and structural arrangement have been associated with perturbations in mitochondrial dynamics and mitophagy [21–23], two critical processes tightly interconnected and responsible for mitochondrial homeostasis [20]. In addition, it is well known that redox balance and mitochondrial dynamics/mitophagy are also phenomena related to each other, as recently demonstrated in fibroblasts from autistic patients [18,39]. Therefore, we focused our attention on the investigation of key components of the mitochondrial fusion and mitophagy machineries in RTT fibroblasts and how they are connected with the above listed deregulated proteins. For this purpose, we decided to complement the proteomic results by evaluating the expression levels of fusion and mitophagy related genes. Jointly, the two approaches can provide a detailed picture of the altered molecular and cellular processes in RTT cells. As shown in Fig. 5, the gene expression levels of mitochondrial fusion components mitofusin 1 (MFN1) and MFN2 were significantly lower in RTT fibroblasts than in control cells. This result parallels with the GO term enrichment analysis, showing significantly down-regulated levels of proteins related to the GO term “mitochondrial organization and biogenesis” (GO:0007005) in RTT fibroblasts.

Mitophagy is an elaborate mitochondrial quality control mechanism required for removing aged and damaged organelles to ensure mitochondrial function and cellular health [20]. In particular, PINK1/Parkin pathway involves the ubiquitination of mitochondrial proteins including mitofusins 1 and 2, which marks mitochondria for mitophagy [20]. As shown in Fig. 5, we observed a significant upregulation of Parkin and PINK1 mRNA levels in RTT fibroblasts as compared to control cells.

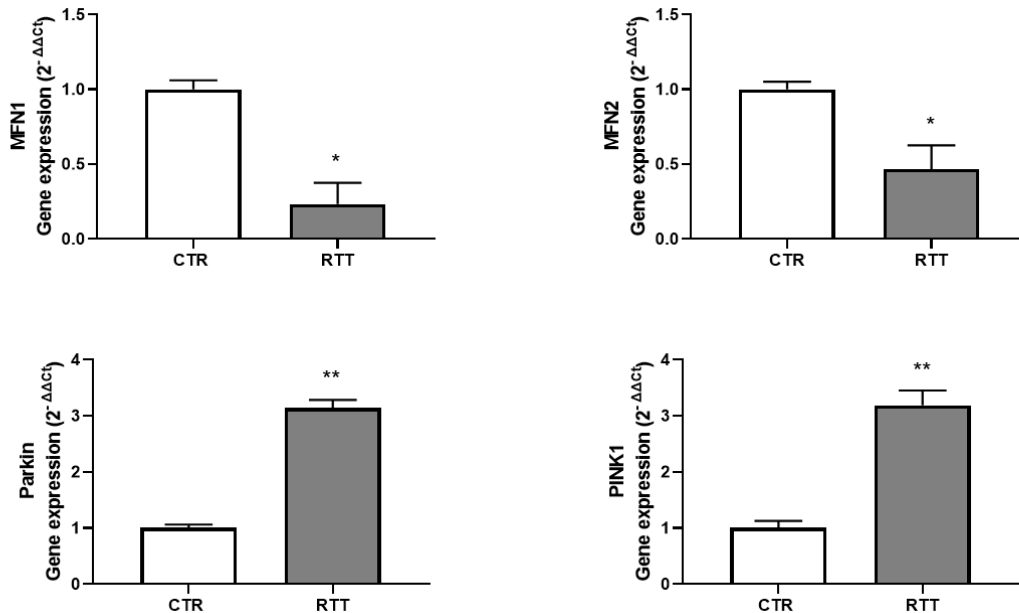


Figure 5. RTT fibroblasts show altered gene expression levels of mitochondrial fusion and mitophagy components. qRT-PCR was performed for genes related to mitochondrial fusion, i.e. MFN1 and MFN2, and mitophagy, i.e. parkin and PINK1. The expression of two fusion genes was significantly lower in RTT fibroblast in comparison to CTR, whereas parkin and PINK1 genes were significantly overexpressed in RTT compared to CTR. The average of CTR samples was set as 1. For each gene, expression levels were normalized to GAPDH using the delta Ct method. Data are represented as mean \pm SEM. p values in relation to CTR were calculated using a Student's t test and set to the following scale: * p < 0.05; ** p < 0.01.

Impaired mitophagy pathway in RTT fibroblasts

In order to further investigate the mitophagy pathway, we also examined the final step in the removal of damaged mitochondria, which consists in the fusion of mitophagosome with lysosome for degradation. Control and RTT fibroblasts were treated with the mitochondrial uncoupling FCCP to induce mitophagy and, then, stained with two different fluorescent dyes specific for mitochondria and lysosomes. As showed in Figure 6, FCCP treatment induced mitophagy in control fibroblasts, as evidenced by the appearance of yellow spots resulting from fusion between mitochondria (red dye) and lysosomes (green dye). On the other hand, RTT cells showed impairment in mitophagy induction after FCCP treatment, as indicated by absence of co-localization between mitochondrial and lysosomal dyes.

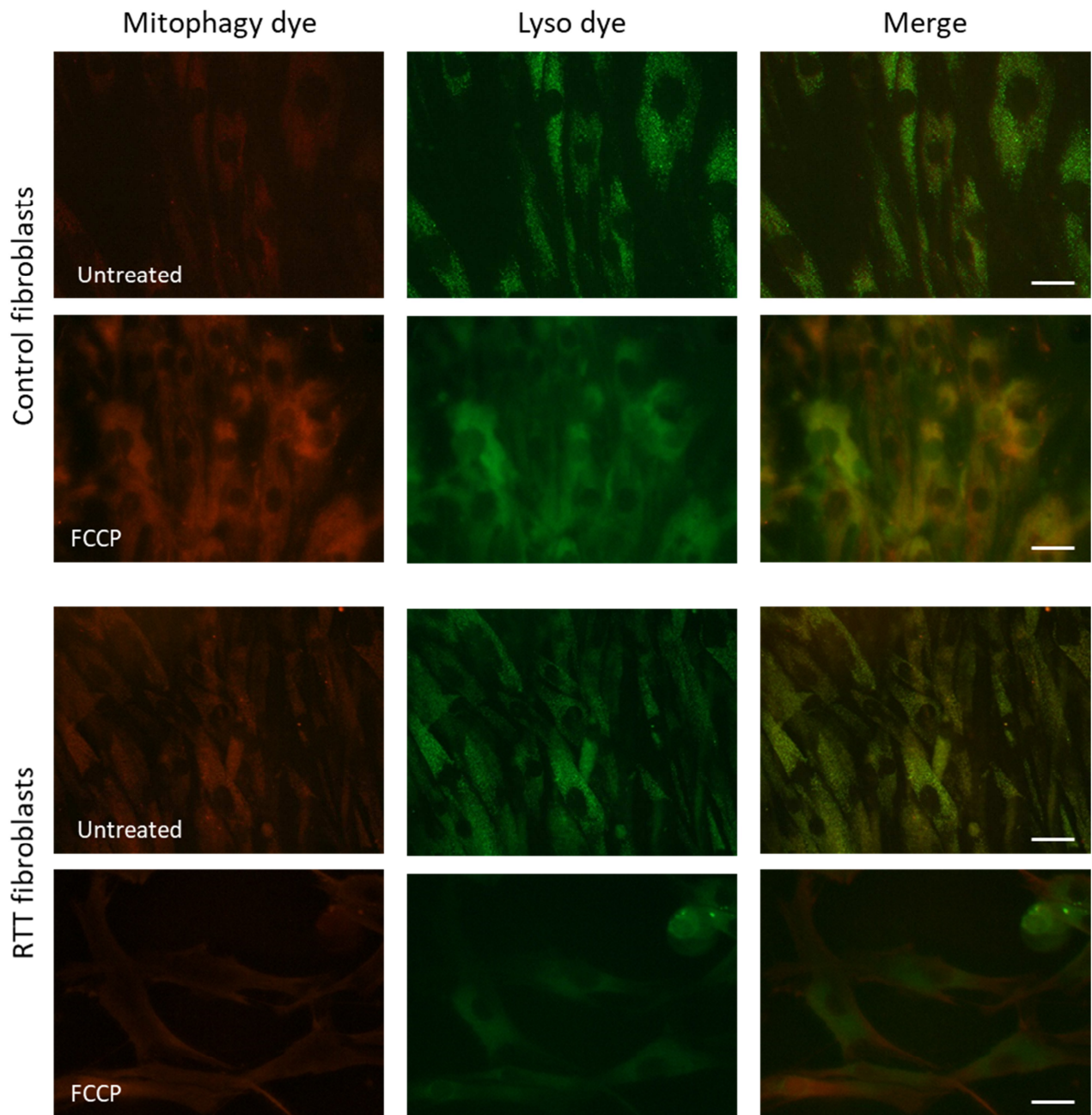


Figure 6. RTT fibroblasts show impaired mitophagy pathway. Representative images of control and RTT fibroblasts untreated or treated with 10 μ M FCCP and co-stained with mitophagy and lysosomal staining dyes. The fluorescent intensity of mitophagy dye was increased in FCCP-treated control cells but not in RTT fibroblasts. In addition, intense yellow color was evident in merge image of treated control cells, indicating co-association between lysosomal and mitochondrial components. No co-localization was noticeable in FCCP-treated RTT fibroblasts, suggesting impairment of mitophagy pathway. Scale bar 20 μ m.

Abnormal ultrastructural morphology in RTT fibroblasts

It is well known that the mitochondrial morphology, size, number and distribution are controlled by a fine-tuned balance of mitochondrial fission-fusion events and mitophagic removal of damaged organelles [20]. Our results seemed to indicate an inadequate mitophagic flux in RTT fibroblasts, probably due to the altered expression of components of mitochondrial dynamics and quality control machinery. Moreover, our proteomic analysis also revealed changes of proteins supporting

mitochondrial structure and biology in RTT fibroblasts (i.e. ATP5MG and COX6B1). Starting from these observations, we therefore decided to investigate the ultrastructure of control and RTT primary dermal fibroblasts. Transmission electron microscopy (TEM) of control fibroblasts showed typical and normal ultrastructural morphology of mitochondria with well-organized lamellar cristae (Fig. 7A-B). On the other hand, ultrastructural examination of RTT fibroblasts revealed evidence of elongated mitochondria with “dissolving” features and electron-dense matrix containing blurry cristae structures (Fig. 7C-D).

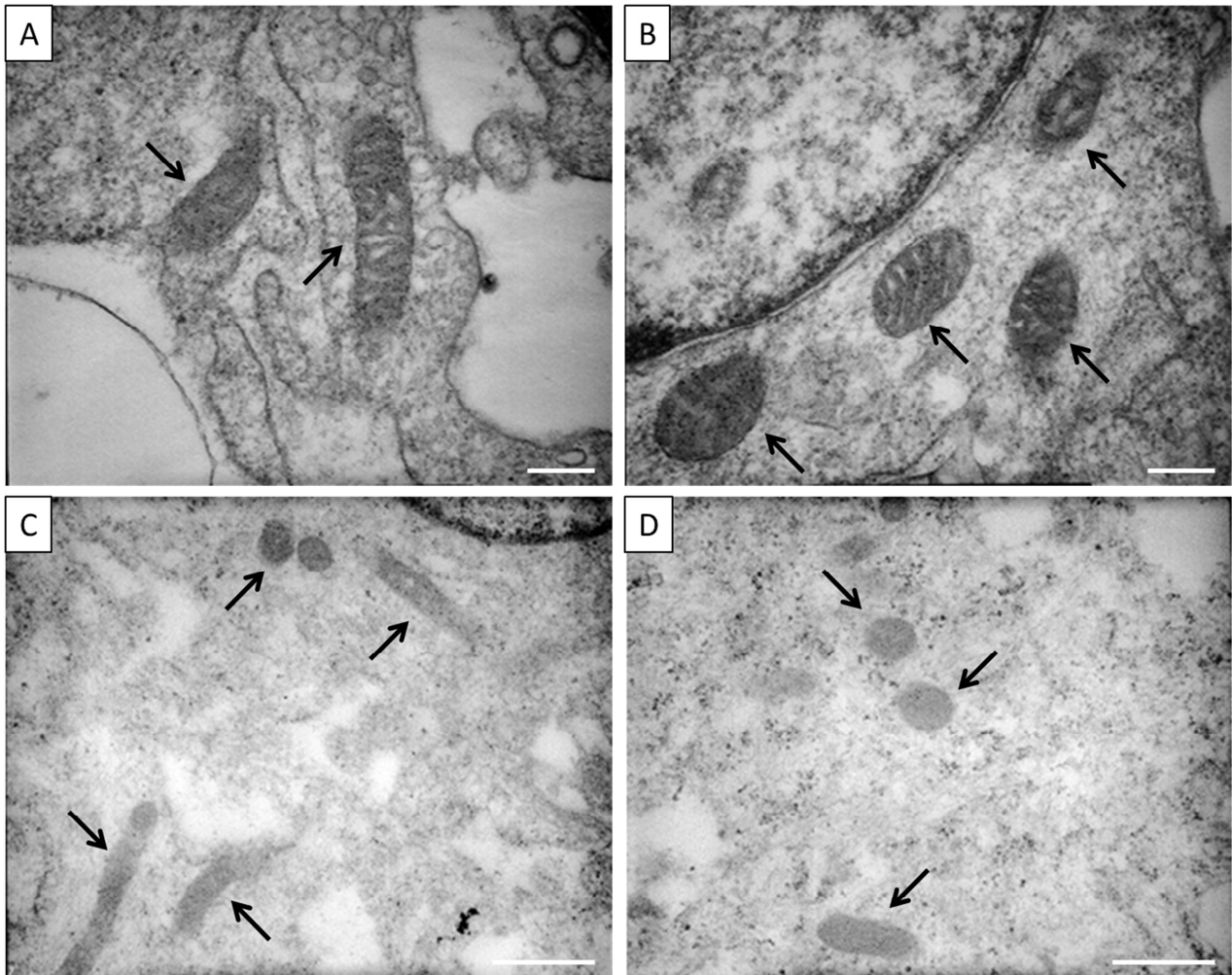


Figure 7. Transmission Electron Microscopy (TEM) analysis of primary dermal fibroblasts from control subjects and RTT patients. (A-B) Representative images of control fibroblasts displaying no ultrastructural alterations. Mitochondria show a well-developed and evenly distributed cristae structure (arrows). (C-D) Ultrastructural morphology of RTT fibroblasts show blurred mitochondria containing damaged or missing cristae (arrows). (A-B) Magnification $\times 50,000$. Scale bar 200 nm. (C-D) Magnification $\times 30,000$. Scale bar 500 nm.

Discussion

Mitochondrial function is recognized as one of the main altered metabolic components in RTT [5]. Atypical mitochondrial morphology, abnormal bioenergetics profile coupled with defects in the enzyme activity of mitochondrial respiratory chain complexes have been described in both humans and experimental animals with RTT [10–13,15–17]. In this regard, a significant part of evidence supporting the link between RTT and mitochondrial dysfunction arises from transcriptomics analysis, showing the altered expression of genes related to mitochondrial pathways [25,26,40,41]. Indeed, based on the transcriptional regulatory function of MeCP2, most studies have focused on understanding the consequences of its mutation on transcriptomic profile to reveal the underlying pathogenetic mechanisms of RTT. However, our understanding of the disease phenotypic manifestations would have greater benefits from the identification of the altered proteome profile resulting from the loss of MeCP2 function. Nevertheless, although its potential significance, changes in protein profile have not yet been widely explored in RTT, except for some studies on human plasma and fibroblasts performed by 2D gel electrophoresis and mass spectrometry, mainly showing oxidative stress and immune imbalance [26–30].

In the present work, we thus performed a comprehensive protein profiling of primary dermal fibroblasts isolated from patients to uncover a profile representing key altered cellular functions associated with RTT phenotype. Our proteomic analysis implicated the identification as well as the qualitative and quantitative assessment of proteins expressed in different cells lines, and clarification of their properties and roles, generally in a large-scale, high-throughput format [42]. The high dimensionality of data generated from this study - in the order of 1,500-2,000 proteins obtained for every sample - required the use of bioinformatics tools and data-mining approaches for efficient and accurate data analysis of CTR and RTT specimens. Mining of such large proteomics data sets allowed us to better understand the complexity of RTT cellular proteome, by providing an in-depth view of the perturbed functional pathways, mainly related to mitochondria, and associated to MeCP2 deficiency. In particular, here, we revealed that RTT fibroblasts are characterized by a distinct proteome signature, which showed a general reduction in the number of proteins implicated in key cellular functions such as cell growth and/or maintenance, energy pathway, protein metabolism and mitochondrial organization/biogenesis. This first finding could be supported by previous evidence indicating a central role for impaired protein synthesis in RTT pathology [43]. In fact, Li and colleagues demonstrated how lack of MeCP2 in mutant neurons was associated with a defect in the global control of transcription resulting in a lower protein synthesis activity also related to a severe defect in AKT/mTOR signaling cascade [43]. Of note, an impaired mitochondrial function with decreased basal and maximal respiration and a reduced expression of mitochondrial-

related genes was also detected in mutant neurons [43]. Conversely, in our RTT cellular model, i.e. dermal fibroblasts, we found a higher percentage of proteins involved in the cellular component “mitochondrion” (GO: 0005739), in particular, proteins related to mitochondrial bioenergetic function and cristae structure as well as proteins involved in the maintenance of cellular redox homeostasis. These data seem to be consistent with our previous microarray analysis performed on RTT PBMC, in which a significant upregulation of transcripts encoding for subunits of mitochondrial respiratory chain complexes and for components of the antioxidant cellular defense system was observed [16]. Given their primary role in cellular energy production, the altered protein expression of cytochrome c oxidase 6B1 and ATP synthase subunit g, subunits of complex IV and V respectively, could affect the ATP-generating process, hypothesis also supported by previous observations of overall suppressed mitochondrial bioenergetics in RTT fibroblasts [10]. Moreover, several studies have also reported evidence for altered expression levels and reduced enzymatic activity of cytochrome c oxidase (complex IV) in muscle and frontal cortex of RTT patients as well as in the skeletal muscle of symptomatic *MeCP2^{tm1Tam}* mouse model [24,34,44]. More recently, *MeCP2* knock-down in primary rat astrocytes was also associated with a decreased enzymatic activity of complex IV that was rescued by quercetin treatment [45]. In addition, ATP synthase protein levels were slightly less expressed in the cortex of *Mecp2^{-y}* mice, but without any difference in the enzymatic activity [46]. Nevertheless, impairment of the ATP synthase function was demonstrated by De Filippis and colleagues in the brain of *Mecp2-308* mouse model [47]. These data could match with our study in which we have found an upregulation of cytochrome c oxidase subunit 6B1 and ATP synthase subunit g, as this could be explained as an attempt by RTT fibroblasts to cope with the deficient activity of the complexes IV and V, but this assumption needs to be confirmed by further investigations.

In addition to providing ATP, mitochondrial complexes are also the main cellular sites for the production of oxidative mediators. Indeed, enzymatic defects of the mitochondrial respiratory chain have been recognized as one of the most relevant triggers of redox imbalance in RTT [10,12]. In this context, our results showing elevated protein expression of NADH-cytochrome b5 reductase 3 and mitochondrial peroxiredoxin-5 clearly fit with the presence of an altered redox homeostasis in RTT [6,7,10,19]. In fact, the two proteins play a central role in cell protection against oxidative stress. In particular, NADH-cytochrome b5 reductase 3 is a redox enzyme linked to the plasma membrane and mitochondria that is able, under cellular stress conditions, to prevent lipid peroxidation damage. Indeed, by providing reductive capacity, NADH-cytochrome b5 reductase 3 preserves antioxidant molecules like coenzyme Q, α -tocopherol, and ascorbate, in their reduced state. Increased activity of NADH-cytochrome b5 reductase 3, associated with an improvement in

mitochondrial function, has been observed in pathological conditions such as aging and age-related diseases [37]. In presence of an impaired mitochondrial activity, the upregulated protein levels of NADH-cytochrome b5 reductase 3 in RTT fibroblasts could represent a compensatory response to contain excessive oxidative insult. As additional role, NADH-cytochrome b5 reductase 3 cooperates with cytochrome b5A (CYB5A) in cellular metabolic pathways such as elongation and desaturation of fatty acids, cholesterol biosynthesis, and xenobiotics metabolism [37]. In this regard, it is interesting to note that, in previous studies, we have detected an upregulation of CYB5A mRNA levels in RTT PBMC and an impaired lipid metabolism in RTT fibroblasts [16,48]. A connection between these two aspects of RTT cells and the increase in NADH-cytochrome b5 reductase 3 protein levels cannot be excluded. Further research directed to investigating its enzymatic activity would allow us to answer this question.

Furthermore, also the levels of another redox-related protein, i.e. mitochondrial peroxiredoxin-5, were significantly upregulated in RTT fibroblasts compared to controls. Within the mitochondrial matrix (but also in cytosol and peroxisomes), peroxiredoxin-5 cooperates with the thioredoxin/thioredoxin reductase/NADPH system in the reduction of H_2O_2 , organic hydroperoxides and peroxynitrite. Based on the generally accepted mechanism of action of this enzyme, the first step implicate the reduction of H_2O_2 with the concomitant formation of a transient intramolecular disulfide bond. Then, the oxidized peroxiredoxin-5 is reduced by the thioredoxin/thioredoxin reductase recycling system to become ready for another catalytic cycle again [49]. Interestingly, in our previous work, we have noticed a reduced activity of thioredoxin reductase in RTT fibroblasts [10]. In this regard, as a compensatory response, RTT cells could attempt to counteract the compromised activity of the recycling system by upregulating peroxiredoxin-5 protein levels. Similarly, we previously showed the upregulation of another member of peroxiredoxin family, i.e. peroxiredoxin-1 whose mRNA levels were upregulated in RTT PBMC [16]. However, the increased protein expression of peroxiredoxin-5 could also depend on its reduced activity. Indeed, it has been shown that post-translational modifications, including acetylation, play a key role in modulating its function with the acetylated form being more active in H_2O_2 -reducing activity [50]. Of note, peroxiredoxins are specific substrates of histone deacetylase 6 (HDAC6), which appears to be involved in RTT neurobiology. Its levels have been found to increase in cells from RTT patients, whereas its inhibition has been shown to improve microtubule dynamics [50]. These results suggested the potential of HDAC6 as an important disease-modifying target in RTT to correct, for example, microtubule-dependent vesicular trafficking of brain-derived neurotrophic factor (BDNF) [50]. In this context, a future study investigating the acetylation status

of peroxiredoxins in RTT cells would be very interesting, also evaluating the therapeutic application of HDAC6 inhibitors to enhance cellular antioxidant activity.

Despite the increased protein expression of NADH-cytochrome b5 reductase 3 and mitochondrial peroxiredoxin-5, it is reasonable to believe that this compensatory antioxidant system is not strong enough to counteract the highly pro-oxidant intracellular milieu of RTT fibroblasts. In fact, we have already demonstrated in RTT an imbalance towards a more oxidative state supported by the combination of a defective enzymatic antioxidant defense coupled with a greater production of ROS, in turn driven by a perturbed mitochondrial function [6,7,10,19]. It is interesting to note that our study showed another important aspect of RTT cells that is the morphological abnormalities of mitochondria. On the one hand, this result is in agreement with previous reports from our group and others [11,12,15], on the other, it reinforces the other data of this investigation and the concept of dysfunctional mitochondria in RTT. Indeed, it is well known the presence of a bidirectional relationship between mitochondrial structure and its functional state and how this can affect the energy supply as well as ROS production [20]. Among the main players involved in regulating the mitochondrial structure/function relationship, we decided to evaluate key components of mitochondrial dynamics and quality control pathways. To our knowledge, this is the first report to reveal the involvement of an altered expression of fusion and mitophagy regulatory factors, including mitofusins and PINK1/Parkin, as a new pathogenic mechanism of RTT. However, it should be noted that a potential role for these pathways in RTT and other neurodevelopmental disorders has already been proposed and, recently, demonstrated in autism by our lab [15,18]. In fact, in a recent study, we reported several mitochondrial abnormalities in autistic fibroblasts such as an altered expression of mitochondrial dynamics/mitophagy regulatory factors and components of electron transport chain together with an overactive bioenergetics profile and an aberrant mitochondrial morphology [18]. Moreover, the presence of redox imbalance and a defective Nrf2 pathway led us to believe that all the changes in mitochondrial function/structure could be compensatory mechanisms that the autistic cells adopt to maintain or support an increased energy demand arising from a chronic oxinflammatory status [18]. Unlike what we observed in autistic cells, in the present study, the possible dysregulation of mitochondrial dynamics and mitophagy could account for the overall suppressed bioenergetic profile, previously noticed in RTT fibroblasts [10,20]. Furthermore, the removal of damaged mitochondria through the mitophagic clearance is a critical process to ensure the cellular homeostasis, especially under oxidative conditions [39]. In our experimental conditions, as a possible consequence of the altered expression of dynamics/mitophagy regulatory factors, in RTT fibroblasts treated with FCCP, the mitophagosomes fail to fuse with the lysosomes to degrade themselves, confirming the inability of these cells to

remove damaged and aged mitochondria. Interestingly, in two recent papers, Sbardella and colleagues demonstrated defects in other intracellular proteolytic processes such as impaired macroautophagy and defective proteasome biogenesis in RTT fibroblasts [51,52]. In particular, under starvation conditions, the inefficient degradation of autophagy substrates such as p62/SQSM1 and 20 S proteasome highlighted the occurrence of a defective autophagic flux in RTT. By TEM analysis, the same authors also documented the retention of mitochondria inside mature red blood cells (RBC) from RTT patients, reinforcing the evidence of impaired autophagy [51]. Furthermore, mitochondria retained into RTT RBC displayed morphological alterations such as a reduced size, an elongated shape and the presence of faint cristae, similarly to what observed in RBC of murine models of defective macroautophagy or mitophagy [51]. In our study, cellular ultrastructure analysis using TEM revealed the presence in RTT cells of similar elongated and blurred mitochondria with the disappearance of cristae structure, supporting the hypothesis that an inefficient mitophagy process could finally lead to the accumulation of damaged and dysfunctional mitochondria also in RTT fibroblasts. On the other hand, mitochondrial cristae, a subcompartment of the inner membrane, play an essential role in the energy-generating process since their morphology determines the assembly and stability of respiratory chain complexes [35]. Therefore, cristae shape alterations can contribute to the suppressed bioenergetic profile observed in RTT cells [10]. It is interesting to note that our study also highlighted the upregulation of one of the many regulators of cristae structure, namely ATP synthase. In fact, in addition to its fundamental role in ATP production, ATP synthase dimers are also involved in maintaining cristae curvature [35]. Importantly, loss of ATP synthase subunit g is associated with major changes in mitochondrial morphology [35]. Therefore, its upregulation could be a compensatory response of RTT fibroblasts to the morphological changes of mitochondria.

In light of these findings, to better understand the molecular basis underlying mitochondrial dysfunction in RTT, a future research in our cellular disease model could be directed to investigate cAMP response element binding protein (CREB), a transcription factor involved, among other functions, in mitochondrial gene expression [53]. In a recent article by Bu and colleagues, mitochondrial alterations - i.e. increased mitochondrial fragmentation and reduced mitochondrial membrane potential – have been associated with reduced CREB signaling in MECP2 mutant neurons differentiated from genetically engineered human stem cell lines. Of note, the pharmacological activation of CREB pathway was able to rescue the above-mentioned mitochondrial phenotype and, in addition, the impairment of neurite growth and dendritic arborization [54]. Based on this evidence, using dermal fibroblasts from the affected patients, which more accurately reflect the real *in vivo* condition, in a future investigation we could shed light on

the possible involvement of CREB signaling pathway in the molecular mechanisms of the mitochondrial alterations detected here, also identifying new potential therapeutic targets for RTT mitochondrial dysfunction.

Conclusions

In this study, mining large proteomics data sets allowed us to explore in-depth the consequences of *MECP2* mutation on the proteome of primary dermal fibroblasts isolated from affected patients. In very few other proteomics studies on RTT samples, the identification of differentially expressed proteins was based on 2-D gel electrophoresis and mass spectrometry analysis that led to a relative low number of identified proteins [26–30]. In addition, most research efforts on RTT so far have focused on transcriptomic analyses [25], but it should be noted that investigations of protein changes might better reflect the pathophysiological mechanisms underlying RTT. Here, thanks to a data mining proteomic approach, we confirmed the pathological relevance of mitochondrial dysregulation in RTT, demonstrating an altered expression of proteins implicated in mitochondrial structure/function pathways as well as in the cellular stress defense. Furthermore, this study provided the first evidence of impaired mitochondrial dynamics and mitophagy in RTT. We propose that these alterations may contribute to the anomalies detected in mitochondrial morphology and ultimately culminate in a compromised metabolic capacity of RTT fibroblasts.

Materials and Methods

Materials

Sodium deoxycholate (SDC), tris(2-carboxyethyl)phosphine (TCEP), iodoacetamide (IAA), formic acid (FA), acetonitrile and ammonium bicarbonate were purchased from Sigma–Aldrich (St. Louis, MO, USA). Pierce-BCA protein assay kit was purchased from Thermo-Fisher (Waltham, Massachusetts, USA). Proteomics sequencing grade modified trypsin was purchased from Promega (Madison, WI, USA).

Subjects population

The subjects enrolled in the study included female patients with clinical diagnosis of typical RTT and *MECP2* mutation (n = 3; median age: 24 +/-12) and healthy controls (n = 2; females, median age: 34 +/- 8). RTT diagnosis and inclusion/exclusion criteria were based on the recently revised RTT nomenclature consensus [55]. All the patients were consecutively admitted to the Child Neuropsychiatry Unit of the “Azienda Ospedaliera Universitaria Senese” (AOUS, Siena, Italy). Samplings from RTT patients were obtained during periodic clinical checkups, while samples in the control group were carried out during routine health checks. This research protocol was carried out in strict compliance with the Helsinki Declaration and conducted with the local Institutional Review Board approval. Written informed consent was obtained from either the parents or legal guardians of all enrolled subjects.

Human skin fibroblast cultures

Human skin fibroblasts were isolated from 3-mm skin punch biopsy (n = 3 for RTT and n = 2 for controls). Skin biopsies were cultured in DMEM, containing 20% fetal bovine serum (FBS) and antibiotics (100 U/ml penicillin, 100 µg/ml streptomycin) at 37°C in a humidified atmosphere containing 5% CO₂. Culture of dermal biopsies continued until the primary growing fibroblasts reached ~ 80% confluence around the explants in culture flasks. Then, the dermal pieces were removed and trypsin/EDTA mixture was added to separate fibroblasts. Cells used in the experiments were grown up-to a maximum of 13 passages.

Preparation of cell culture samples

Cell cultures were lysed with a solution of 2% SDC/100 mM ammonium bicarbonate. The cell lysates were reduced with 5 mM TCEP at 60°C for 30 min and alkylated in the dark with 10 mM IAA at room temperature for 30 min. Protein quantification was performed using BCA assay following manufacturers' instructions. 60 µg of proteins, for each sample, were processed adding trypsin using an enzyme-to-protein ratio of 1:40 and incubated at 37°C overnight. Following digestion, all reaction mixtures were acidified with 1% FA in order to inhibit any remaining enzyme activity and to precipitate the SDC [56,57].

Digested samples were desalted using OASIS cartridges (Waters), brought to dryness and reconstituted in 0.1% formic acid in water/acetonitrile (97/3, v/v). LC-MS/MS analyses were performed using Q-Exactive Plus Orbitrap mass spectrometer (Thermo Scientific). The peptide separation was carried out at 50°C using a Acquity UPLC™ peptide CSH C₁₈ column, 1mm x 100mm, 1.7 μm, 130 Å (Waters) at a flow rate of 100 μl/min. The mobile phases A and B used for the analysis were 0.1% formic acid in water and 0.1% formic acid in acetonitrile respectively. The gradient started with 3% of B and then it was increased up to 90 % in 230 minutes. These experiments were performed using a DDA setting to select the “top twelve” most-abundant ions for MS/MS analysis. Protein identification was performed using Proteome Discover (Thermo Scientific) and Sequest algorithm.

The output of a proteome analysis is typically a long list of identified factors, that have a probability score and ideally also a quantitative value associated with them. In order to understand and decipher these data and to generate testable hypothesis, the list has to be further classified and filtered. Functional annotation analysis was carried out using DAVID 6.8 [58], an integrated biological knowledgebase and analytic tool aimed at systematically extracting biological meaning from large gene/protein lists. The first step for a functional analysis of a large protein list is to connect the protein name to a unique identifier. This is the reason why protein list was submitted through DAVID 6.8 panel and “UNIPROT ACCESSION” was selected as identifier name. The input protein list completely mapped to the internal DAVID IDs and belonged to *Homo sapiens*. For a functional interpretation of the results, the protein identifiers are associated to its related Gene Ontology (GO) terms [59] overcoming the redundancy in terminology for “biological process”, “molecular function” or “cellular component” [60]. After a GO-term annotation, a GO-term enrichment analysis was performed to compare the abundance of specific GO-terms in the dataset with the natural abundance in a reference dataset [61]. To extract functions that are significantly enriched in the target set in comparison to a reference set, a p-value is calculated to show overrepresentation of a specific GO term. Beyond the use of DAVID online tool, another bioinformatics software, FunRich 3.1.3, [62] was applied in this study for confirming results and for a graphical description of enrichment and network analysis. String version 11.0 was used to verify the shell of interactors of specific proteins [63].

The default peak-picking settings were used to process the raw MS files in MaxQuant [64] (version 1.6.1.0) and its integrated search engine Andromeda [65]. Protein identification and label free quantification (LFQ) by MaxQuant/Andromeda was based on at least one unique peptide with a minimum length of seven amino acids and a false discovery rate of 0.01 applied to both peptide and protein level. ‘Advanced ratio estimation’ was on. Match time window size was by default 0.7 min,

and alignment time window size was 20 min. FDR of 0.01 was set as a threshold for peptide and protein identifications. MaxQuant automatically aligned the runs.

For processing of MaxQuant result files (that is, the 'proteinGroups.txt' file), the freely available software Perseus (version 1.6.1.1) was used to compare the peak intensities across the whole set of measurements to obtain quantitative data for all of the peptides in the sample. Proteins identified from the reverse sequence database or based on a single modified peptide, as well as non-human contaminant proteins identified from the contaminant sequence database, were filtered out. The LFQ intensities of proteins from the MaxQuant analysis were imported and transformed to logarithmic scale with base two. The missing values were replaced (imputed) with the value of the lowest intensity. The protein quantification and calculation of statistical significance was carried out using two-way Student-t test and error correction (p value < 0.05) with the method of Benjamini-Hochberg. For further visualization, a Principle component analysis (PCA) were performed. PCA is a way to investigate underlying differences between samples and replicates in quantitative proteomics results [66]. It is used for multivariate analysis of proteome dynamics based on both protein abundance and turnover information generated by mass spectrometry. PCA is responsible for separating features into groups based on commonality and reports the weight of each component's contribution to the separation. The mechanism underlying PCA is an orthogonal transformation transferring a set of correlated variables into a new set of uncorrelated variables.

Moreover, volcano plots were used to show a summary distribution of differentially expressed proteins between RTT and CTR samples. The volcano plot is an easy-to-interpret scatter plot that arranges values along dimensions of biological (difference RTT and CTR) and statistical (log₁₀ p-value) significance. The proteins located on the upper left region and the upper right region (difference A-C and B-C >±2, FDR<0.05) are differentially expressed.

Reverse transcription quantitative polymerase chain reaction (RT-qPCR)

Total RNA was extracted from fibroblasts using the RNeasy mini kit (Qiagen, Hilden, Germany) and RT-qPCR was performed as previously reported [17]. Primer sequences used for analysis of gene expression are as follows: MFN1 fwd, 5'- CCTCCTCTCCGCCTTAACT -3'; MFN1 rev, 5'- TATGCTAAGTCTCCGCTCCA -3'; MFN2 fwd, 5'- GCCAACCTCAACCTGAGACA -3'; MFN2 rev, 5'- GAGCAGGGACATTGCGTTTT -3'; PINK1 fwd, 5'- ATGTGGAACATCTCGGCAGG -3'; PINK1 rev, 5'- TGACTGCTCCATACTCCCA -3'; Parkin fwd, 5'- TAAGCGGAGTTTCAGCCACA -3'; Parkin rev, 5'- ACCTGACAAACACTGTAATTGGA-3'; GAPDH fwd, 5'- TCGGAGTCAACGGATTTGGT -3'; GAPDH rev, 5'- TTCCCGTTCTCAGCCTTGAC -3'. After normalization to more stable GAPDH mRNA, the folds

of variation were determined with respect to the control, using the formula $2^{-\Delta\Delta Ct}$, where ΔCt is (gene of interest Ct) – (GAPDH Ct) and $\Delta\Delta Ct$ is (ΔCt experimental) – (ΔCt control).

Mitophagy detection

Mitophagy was detected using a commercial mitophagy detection kit (catalog no. MD01–10; Dojindo Molecular Technologies, Inc., Kumamoto, Japan). Briefly, cells were seeded on coverslips and cultured overnight. Fibroblasts were washed twice with Hanks' HEPES buffer and then incubated with Mtpagy Dye solution for 30 min. Cells were washed and treated with 10 μ M FCCP. After incubation for 24 h, cells were incubated with Lyso Dye solution at 37°C for 30 min. Then, the cells were washed twice and the co-localization of Mtpagy and Lyso Dyes was observed with a fluorescence microscopy (Nikon Microphot FXA microscope).

Transmission electron microscopy

Ultrastructural analysis of fibroblasts was performed as previously reported [17]. Briefly, cells were fixed in 2.5% glutaraldehyde in 0.1 M sodium cacodylate buffer for 4 h at 4°C. Then, cells were post-fixed in 1% osmium tetroxide for 2 h at 4 °C, dehydrated in graded concentrations of ethanol, embedded in epoxide resin, and polymerized in oven at 60 °C for 48 h. Ultrathin sections of 60 nm were cut using an ultramicrotome (Ultratome Reichert SuperNova Leica, Wien, Austria), stained with 1% uranyl acetate and 0.1% lead citrate for 30 min each and examined under a transmission electron microscope, Hitachi H-800 (Tokyo, Japan).

Statistical analysis

Statistical analysis was performed using GraphPad Prism software. For all the variables tested, Student-t test was used. Statistical significance was indicated by a P-value <0.05. Data were expressed as mean \pm SEM from triplicate determinations obtained in three separate experiments.

References

- [1] R.E. Amir, I.B. Van den Veyver, M. Wan, C.Q. Tran, U. Francke, H.Y. Zoghbi, Rett syndrome is caused by mutations in X-linked MECP2, encoding methyl-CpG-binding protein 2, *Nature Genetics*. 23 (1999) 185–188. <https://doi.org/10.1038/13810>.
- [2] M. Chahrour, H.Y. Zoghbi, The Story of Rett Syndrome: From Clinic to Neurobiology, *Neuron*. 56 (2007) 422–437. <https://doi.org/10.1016/j.neuron.2007.10.001>.
- [3] B. Hagberg, Clinical manifestations and stages of Rett syndrome, *Ment Retard Dev Disabil Res Rev*. 8 (2002) 61–65. <https://doi.org/10.1002/mrdd.10020>.
- [4] H. Yang, K. Li, S. Han, A. Zhou, Z.J. Zhou, Leveraging the genetic basis of Rett syndrome to ascertain pathophysiology, *Neurobiol Learn Mem*. 165 (2019) 106961. <https://doi.org/10.1016/j.nlm.2018.11.006>.
- [5] S.M. Kyle, N. Vashi, M.J. Justice, Rett syndrome: a neurological disorder with metabolic components, *Open Biol*. 8 (2018). <https://doi.org/10.1098/rsob.170216>.
- [6] G. Valacchi, A. Pecorelli, C. Cervellati, J. Hayek, 4-hydroxynonenal protein adducts: Key mediator in Rett syndrome oxinflammation, *Free Radical Biology and Medicine*. 111 (2017) 270–280. <https://doi.org/10.1016/j.freeradbiomed.2016.12.045>.
- [7] A. Pecorelli, C. Cervellati, J. Hayek, G. Valacchi, OxInflammation in Rett syndrome, *The International Journal of Biochemistry & Cell Biology*. 81 (2016) 246–253. <https://doi.org/10.1016/j.biocel.2016.07.015>.
- [8] G. Valacchi, F. Virgili, C. Cervellati, A. Pecorelli, OxInflammation: From Subclinical Condition to Pathological Biomarker, *Front Physiol*. 9 (2018). <https://doi.org/10.3389/fphys.2018.00858>.
- [9] A. Pecorelli, C. Cervellati, V. Cordone, J. Hayek, G. Valacchi, Compromised immune/inflammatory responses in Rett syndrome, *Free Radical Biology and Medicine*. (2020). <https://doi.org/10.1016/j.freeradbiomed.2020.02.023>.
- [10] C. Cervellati, C. Sticozzi, A. Romani, G. Belmonte, D. De Rasmo, A. Signorile, F. Cervellati, C. Milanese, P.G. Mastroberardino, A. Pecorelli, V. Savelli, H.J. Forman, J. Hayek, G. Valacchi, Impaired enzymatic defensive activity, mitochondrial dysfunction and proteasome activation are involved in RTT cell oxidative damage, *Biochimica et Biophysica Acta (BBA) - Molecular Basis of Disease*. 1852 (2015) 2066–2074. <https://doi.org/10.1016/j.bbadis.2015.07.014>.
- [11] S. Filosa, A. Pecorelli, M. D'Esposito, G. Valacchi, J. Hajek, Exploring the possible link between MeCP2 and oxidative stress in Rett syndrome, *Free Radical Biology and Medicine*. 88 (2015) 81–90. <https://doi.org/10.1016/j.freeradbiomed.2015.04.019>.
- [12] N. Shulyakova, A.C. Andreatza, L.R. Mills, J.H. Eubanks, Mitochondrial Dysfunction in the Pathogenesis of Rett Syndrome: Implications for Mitochondria-Targeted Therapies, *Front Cell Neurosci*. 11 (2017). <https://doi.org/10.3389/fncel.2017.00058>.
- [13] M. Müller, K. Can, Aberrant redox homeostasis and mitochondrial dysfunction in Rett syndrome, *Biochem. Soc. Trans*. 42 (2014) 959–964. <https://doi.org/10.1042/BST20140071>.
- [14] Y. Chen, Z. Zhou, W. Min, Mitochondria, Oxidative Stress and Innate Immunity, *Front Physiol*. 9 (2018). <https://doi.org/10.3389/fphys.2018.01487>.
- [15] D. Valenti, L. de Bari, B. De Filippis, A. Henrion-Caude, R.A. Vacca, Mitochondrial dysfunction as a central actor in intellectual disability-related diseases: An overview of Down syndrome, autism, Fragile X and Rett syndrome, *Neuroscience & Biobehavioral Reviews*. 46 (2014) 202–217. <https://doi.org/10.1016/j.neubiorev.2014.01.012>.
- [16] A. Pecorelli, G. Leoni, F. Cervellati, R. Canali, C. Signorini, S. Leoncini, A. Cortelazzo, C. De Felice, L. Ciccoli, J. Hayek, G. Valacchi, Genes Related to Mitochondrial Functions, Protein Degradation, and Chromatin Folding Are Differentially Expressed in Lymphomonocytes of Rett Syndrome Patients, *Mediators Inflamm*. 2013 (2013). <https://doi.org/10.1155/2013/137629>.

- [17] A. Pecorelli, F. Cervellati, G. Belmonte, G. Montagner, P. Waldon, J. Hayek, R. Gambari, G. Valacchi, Cytokines profile and peripheral blood mononuclear cells morphology in Rett and autistic patients, *Cytokine*. 77 (2016) 180–188. <https://doi.org/10.1016/j.cyto.2015.10.002>.
- [18] A. Pecorelli, F. Ferrara, N. Messano, V. Cordone, M.L. Schiavone, F. Cervellati, B. Woodby, C. Cervellati, J. Hayek, G. Valacchi, Alterations of mitochondrial bioenergetics, dynamics, and morphology support the theory of oxidative damage involvement in autism spectrum disorder, *FASEB J*. 34 (2020) 6521–6538. <https://doi.org/10.1096/fj.201902677R>.
- [19] V. Cordone, A. Pecorelli, F. Amicarelli, J. Hayek, G. Valacchi, The complexity of Rett syndrome models: Primary fibroblasts as a disease-in-a-dish reliable approach, *Drug Discovery Today: Disease Models*. (2019). <https://doi.org/10.1016/j.ddmod.2019.11.001>.
- [20] S.B. Yu, G. Pekkurnaz, Mechanisms Orchestrating Mitochondrial Dynamics for Energy Homeostasis, *Journal of Molecular Biology*. 430 (2018) 3922–3941. <https://doi.org/10.1016/j.jmb.2018.07.027>.
- [21] S. Franco-Iborra, M. Vila, C. Perier, Mitochondrial Quality Control in Neurodegenerative Diseases: Focus on Parkinson’s Disease and Huntington’s Disease, *Front. Neurosci*. 12 (2018). <https://doi.org/10.3389/fnins.2018.00342>.
- [22] S. Nobis, A. Goichon, N. Achamrah, C. Guérin, S. Azhar, P. Chan, A. Morin, C. Bôle-Feysot, J.C. do Rego, D. Vaudry, P. Déchelotte, L. Belmonte, M. Coëffier, Alterations of proteome, mitochondrial dynamic and autophagy in the hypothalamus during activity-based anorexia, *Scientific Reports*. 8 (2018) 1–15. <https://doi.org/10.1038/s41598-018-25548-9>.
- [23] K.L. Stauch, P.R. Purnell, H.S. Fox, Aging synaptic mitochondria exhibit dynamic proteomic changes while maintaining bioenergetic function, *Aging (Albany NY)*. 6 (2014) 320–334.
- [24] W.A. Gold, S.L. Williamson, S. Kaur, I.P. Hargreaves, J.M. Land, G.J. Pelka, P.P.L. Tam, J. Christodoulou, Mitochondrial dysfunction in the skeletal muscle of a mouse model of Rett syndrome (RTT): implications for the disease phenotype, *Mitochondrion*. 15 (2014) 10–17. <https://doi.org/10.1016/j.mito.2014.02.012>.
- [25] S. Shovlin, D. Tropea, Transcriptome level analysis in Rett syndrome using human samples from different tissues, *Orphanet J Rare Dis*. 13 (2018). <https://doi.org/10.1186/s13023-018-0857-8>.
- [26] R. Krishnaraj, F. Haase, B. Coorey, E.J. Luca, I. Wong, A. Boyling, C. Ellaway, J. Christodoulou, W.A. Gold, Genome-wide transcriptomic and proteomic studies of Rett syndrome mouse models identify common signaling pathways and cellular functions as potential therapeutic targets, *Human Mutation*. 40 (2019) 2184–2196. <https://doi.org/10.1002/humu.23887>.
- [27] N.L. Pacheco, M.R. Heaven, L.M. Holt, D.K. Crossman, K.J. Boggio, S.A. Shaffer, D.L. Flint, M.L. Olsen, RNA sequencing and proteomics approaches reveal novel deficits in the cortex of *Mecp2*-deficient mice, a model for Rett syndrome, *Mol Autism*. 8 (2017). <https://doi.org/10.1186/s13229-017-0174-4>.
- [28] A. Pecorelli, C. Cervellati, A. Cortelazzo, F. Cervellati, C. Sticozzi, C. Mirasole, R. Guerranti, A. Trentini, L. Zolla, V. Savelli, J. Hayek, G. Valacchi, Proteomic analysis of 4-hydroxynonenal and nitrotyrosine modified proteins in RTT fibroblasts, *The International Journal of Biochemistry & Cell Biology*. 81 (2016) 236–245. <https://doi.org/10.1016/j.biocel.2016.08.001>.
- [29] A. Cortelazzo, C. De Felice, R. Guerranti, C. Signorini, S. Leoncini, A. Pecorelli, G. Zollo, C. Landi, G. Valacchi, L. Ciccoli, L. Bini, J. Hayek, Subclinical Inflammatory Status in Rett Syndrome, *Mediators of Inflammation*. 2014 (2014) 1–13. <https://doi.org/10.1155/2014/480980>.
- [30] A. Cortelazzo, R. Guerranti, C. De Felice, C. Signorini, S. Leoncini, A. Pecorelli, C. Landi, L. Bini, B. Montomoli, C. Sticozzi, L. Ciccoli, G. Valacchi, J. Hayek, A Plasma Proteomic Approach in Rett Syndrome: Classical versus Preserved Speech Variant, *Mediators of Inflammation*. (2013). <https://doi.org/10.1155/2013/438653>.

- [31] P. Sinitcyn, J.D. Rudolph, J. Cox, Computational Methods for Understanding Mass Spectrometry–Based Shotgun Proteomics Data, *Annual Review of Biomedical Data Science*. 1 (2018) 207–234. <https://doi.org/10.1146/annurev-biodatasci-080917-013516>.
- [32] H. Mi, A. Muruganujan, D. Ebert, X. Huang, P.D. Thomas, PANTHER version 14: more genomes, a new PANTHER GO-slim and improvements in enrichment analysis tools, *Nucleic Acids Res.* 47 (2019) D419–D426. <https://doi.org/10.1093/nar/gky1038>.
- [33] S. Kriaucionis, A. Paterson, J. Curtis, J. Guy, N. Macleod, A. Bird, Gene expression analysis exposes mitochondrial abnormalities in a mouse model of Rett syndrome, *Mol. Cell. Biol.* 26 (2006) 5033–5042. <https://doi.org/10.1128/MCB.01665-05>.
- [34] J.H. Gibson, B. Slobedman, H. K N, S.L. Williamson, D. Minchenko, A. El-Osta, J.L. Stern, J. Christodoulou, Downstream targets of methyl CpG binding protein 2 and their abnormal expression in the frontal cortex of the human Rett syndrome brain, *BMC Neurosci.* 11 (2010) 53. <https://doi.org/10.1186/1471-2202-11-53>.
- [35] N. Baker, J. Patel, M. Khacho, Linking mitochondrial dynamics, cristae remodeling and supercomplex formation: How mitochondrial structure can regulate bioenergetics, *Mitochondrion*. (2019). <https://doi.org/10.1016/j.mito.2019.06.003>.
- [36] S. Zong, M. Wu, J. Gu, T. Liu, R. Guo, M. Yang, Structure of the intact 14-subunit human cytochrome c oxidase, *Cell Res.* 28 (2018) 1026–1034. <https://doi.org/10.1038/s41422-018-0071-1>.
- [37] E. Siendones, M. Ballesteros, P. Navas, Cellular and Molecular Mechanisms of Recessive Hereditary Methaemoglobinemia Type II, *J Clin Med.* 7 (2018). <https://doi.org/10.3390/jcm7100341>.
- [38] G. Detienne, W. De Haes, L. Mergan, S.L. Edwards, L. Temmerman, S. Van Bael, Beyond ROS clearance: Peroxiredoxins in stress signaling and aging, *Ageing Research Reviews*. 44 (2018) 33–48. <https://doi.org/10.1016/j.arr.2018.03.005>.
- [39] P.H.G.M. Willems, R. Rossignol, C.E.J. Dieteren, M.P. Murphy, W.J.H. Koopman, Redox Homeostasis and Mitochondrial Dynamics, *Cell Metabolism*. 22 (2015) 207–218. <https://doi.org/10.1016/j.cmet.2015.06.006>.
- [40] M. Aldosary, A. Al-Bakheet, H. Al-Dhalaan, R. Almass, M. Alsagob, B. Al-Younes, L. AlQuait, O.M. Mustafa, M. Bulbul, Z. Rahbeeni, M. Alfadhel, A. Chedrawi, Z. Al-Hassnan, M. AlDosari, H. Al-Zaidan, M.A. Al-Muhaizea, M.D. AlSayed, M.A. Salih, M. AlShammari, M. Faiyaz-Ul-Haque, M.A. Chishti, O. Al-Harazi, A. Al-Odaib, N. Kaya, D. Colak, Rett Syndrome, a Neurodevelopmental Disorder, Whole-Transcriptome, and Mitochondrial Genome Multiomics Analyses Identify Novel Variations and Disease Pathways, *OMICS*. 24 (2020) 160–171. <https://doi.org/10.1089/omi.2019.0192>.
- [41] A. Sanfeliu, K. Hokamp, M. Gill, D. Tropea, Transcriptomic Analysis of Mecp2 Mutant Mice Reveals Differentially Expressed Genes and Altered Mechanisms in Both Blood and Brain, *Front Psychiatry*. 10 (2019). <https://doi.org/10.3389/fpsyt.2019.00278>.
- [42] A. Haoudi, H. Bensmail, Bioinformatics and data mining in proteomics, *Expert Review of Proteomics*. 3 (2006) 333–343. <https://doi.org/10.1586/14789450.3.3.333>.
- [43] Y. Li, H. Wang, J. Muffat, A.W. Cheng, D.A. Orlando, J. Lovén, S. Kwok, D.A. Feldman, H.S. Bateup, Q. Gao, D. Hockemeyer, M. Mitalipova, C.A. Lewis, M.G. Vander Heiden, M. Sur, R.A. Young, R. Jaenisch, Global transcriptional and translational repression in human embryonic stem cells-derived Rett Syndrome neurons, *Cell Stem Cell*. 13 (2013) 446–458. <https://doi.org/10.1016/j.stem.2013.09.001>.
- [44] S.B. Coker, A.R. Melnyk, Rett Syndrome and Mitochondrial Enzyme Deficiencies, *J Child Neurol*. 6 (1991) 164–166. <https://doi.org/10.1177/088307389100600216>.
- [45] A. Dave, F. Shukla, H. Wala, P. Pillai, Mitochondrial Electron Transport Chain Complex Dysfunction in MeCP2 Knock-Down Astrocytes: Protective Effects of Quercetin Hydrate, *J Mol Neurosci*. 67 (2019) 16–27. <https://doi.org/10.1007/s12031-018-1197-9>.

- [46] K. Can, C. Menzfeld, L. Rinne, P. Rehling, S. Kügler, G. Golubiani, J. Dudek, M. Müller, Neuronal Redox-Imbalance in Rett Syndrome Affects Mitochondria as Well as Cytosol, and Is Accompanied by Intensified Mitochondrial O₂ Consumption and ROS Release, *Front Physiol.* 10 (2019). <https://doi.org/10.3389/fphys.2019.00479>.
- [47] B. De Filippis, D. Valenti, L. de Bari, D. De Rasmio, M. Musto, A. Fabbri, L. Ricceri, C. Fiorentini, G. Laviola, R.A. Vacca, Mitochondrial free radical overproduction due to respiratory chain impairment in the brain of a mouse model of Rett syndrome: protective effect of CNF1, *Free Radical Biology and Medicine.* 83 (2015) 167–177. <https://doi.org/10.1016/j.freeradbiomed.2015.02.014>.
- [48] C. Sticozzi, G. Belmonte, A. Pecorelli, F. Cervellati, S. Leoncini, C. Signorini, L. Ciccoli, C.D. Felice, J. Hayek, G. Valacchi, Scavenger receptor B1 post-translational modifications in Rett syndrome, *FEBS Letters.* 587 (2013) 2199–2204. <https://doi.org/10.1016/j.febslet.2013.05.042>.
- [49] J. Lu, A. Holmgren, The thioredoxin antioxidant system, *Free Radical Biology and Medicine.* 66 (2014) 75–87. <https://doi.org/10.1016/j.freeradbiomed.2013.07.036>.
- [50] M. Brindisi, A.P. Saraswati, S. Brogi, S. Gemma, S. Butini, G. Campiani, Old but Gold: Tracking the New Guise of Histone Deacetylase 6 (HDAC6) Enzyme as a Biomarker and Therapeutic Target in Rare Diseases, *J. Med. Chem.* 63 (2020) 23–39. <https://doi.org/10.1021/acs.jmedchem.9b00924>.
- [51] D. Sbardella, G.R. Tundo, L. Campagnolo, G. Valacchi, A. Orlandi, P. Curatolo, G. Borsellino, M. D'Esposito, C. Ciaccio, S.D. Cesare, D.D. Pierro, C. Galasso, M.E. Santarone, J. Hayek, M. Coletta, S. Marini, Retention of Mitochondria in Mature Human Red Blood Cells as the Result of Autophagy Impairment in Rett Syndrome, *Scientific Reports.* 7 (2017) 1–12. <https://doi.org/10.1038/s41598-017-12069-0>.
- [52] D. Sbardella, G.R. Tundo, V. Cunsolo, G. Grasso, R. Cascella, V. Caputo, A.M. Santoro, D. Milardi, A. Pecorelli, C. Ciaccio, D. Di Pierro, S. Leoncini, L. Campagnolo, V. Pironi, F. Oddone, P. Manni, S. Foti, E. Giardina, C. De Felice, J. Hayek, P. Curatolo, C. Galasso, G. Valacchi, M. Coletta, G. Graziani, S. Marini, Defective proteasome biogenesis into skin fibroblasts isolated from Rett syndrome subjects with MeCP2 non-sense mutations, *Biochimica et Biophysica Acta (BBA) - Molecular Basis of Disease.* 1866 (2020) 165793. <https://doi.org/10.1016/j.bbadis.2020.165793>.
- [53] D. De Rasmio, A. Signorile, E. Roca, S. Papa, cAMP response element-binding protein (CREB) is imported into mitochondria and promotes protein synthesis, *FEBS J.* 276 (2009) 4325–4333. <https://doi.org/10.1111/j.1742-4658.2009.07133.x>.
- [54] Q. Bu, A. Wang, H. Hamzah, A. Waldman, K. Jiang, Q. Dong, R. Li, J. Kim, D. Turner, Q. Chang, CREB Signaling Is Involved in Rett Syndrome Pathogenesis, *J. Neurosci.* 37 (2017) 3671–3685. <https://doi.org/10.1523/JNEUROSCI.3735-16.2017>.
- [55] J.L. Neul, W.E. Kaufmann, D.G. Glaze, J. Christodoulou, A.J. Clarke, N. Bahi-Buisson, H. Leonard, M.E.S. Bailey, N.C. Schanen, M. Zappella, A. Renieri, P. Huppke, A.K. Percy, RettSearch Consortium, Rett syndrome: revised diagnostic criteria and nomenclature, *Ann. Neurol.* 68 (2010) 944–950. <https://doi.org/10.1002/ana.22124>.
- [56] Y. Lin, J. Zhou, D. Bi, P. Chen, X. Wang, S. Liang, Sodium-deoxycholate-assisted tryptic digestion and identification of proteolytically resistant proteins, *Anal. Biochem.* 377 (2008) 259–266. <https://doi.org/10.1016/j.ab.2008.03.009>.
- [57] J. Zhou, T. Zhou, R. Cao, Z. Liu, J. Shen, P. Chen, X. Wang, S. Liang, Evaluation of the application of sodium deoxycholate to proteomic analysis of rat hippocampal plasma membrane, *J. Proteome Res.* 5 (2006) 2547–2553. <https://doi.org/10.1021/pr060112a>.
- [58] D.W. Huang, B.T. Sherman, R.A. Lempicki, Bioinformatics enrichment tools: paths toward the comprehensive functional analysis of large gene lists, *Nucleic Acids Res.* 37 (2009) 1–13. <https://doi.org/10.1093/nar/gkn923>.

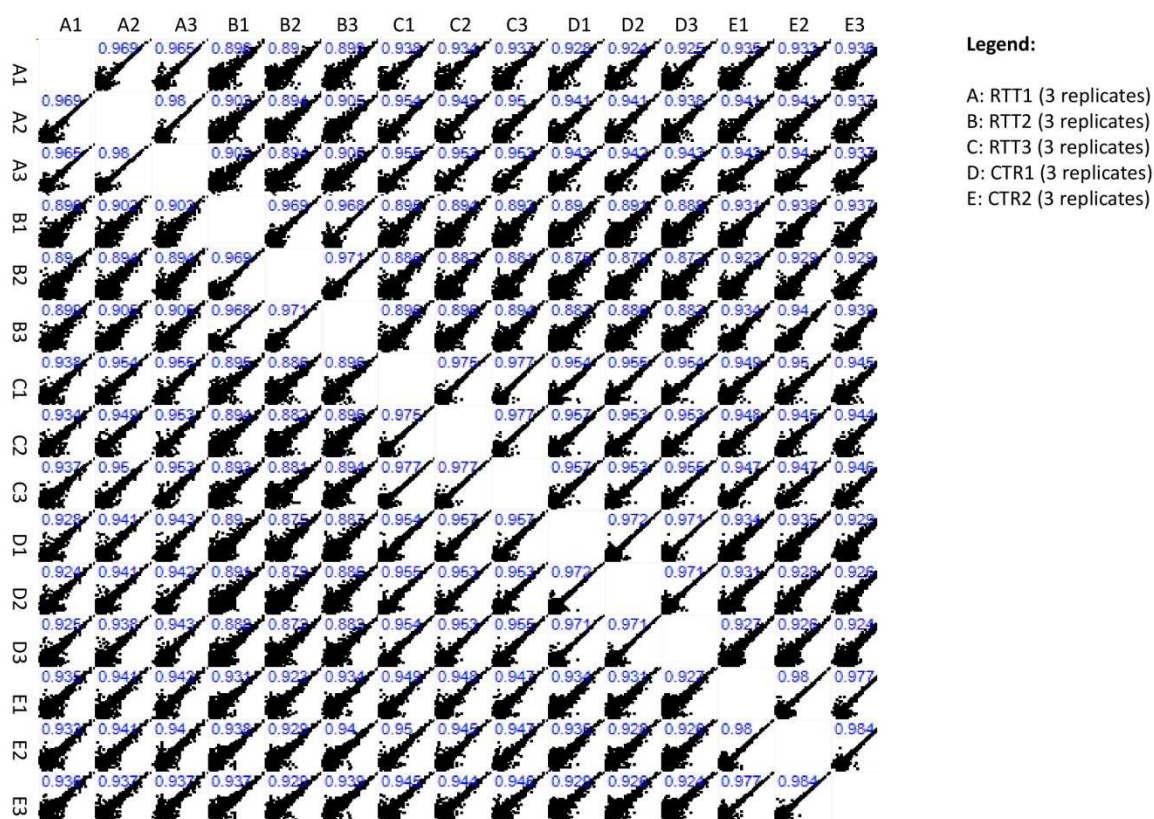
- [59] M. Ashburner, C.A. Ball, J.A. Blake, D. Botstein, H. Butler, J.M. Cherry, A.P. Davis, K. Dolinski, S.S. Dwight, J.T. Eppig, M.A. Harris, D.P. Hill, L. Issel-Tarver, A. Kasarskis, S. Lewis, J.C. Matese, J.E. Richardson, M. Ringwald, G.M. Rubin, G. Sherlock, Gene ontology: tool for the unification of biology. The Gene Ontology Consortium, *Nat. Genet.* 25 (2000) 25–29. <https://doi.org/10.1038/75556>.
- [60] S. Yon Rhee, V. Wood, K. Dolinski, S. Draghici, Use and misuse of the gene ontology annotations, *Nature Reviews Genetics.* 9 (2008) 509–515. <https://doi.org/10.1038/nrg2363>.
- [61] R. Malik, K. Dulla, E.A. Nigg, R. Körner, From proteome lists to biological impact--tools and strategies for the analysis of large MS data sets, *Proteomics.* 10 (2010) 1270–1283. <https://doi.org/10.1002/pmic.200900365>.
- [62] M. Pathan, S. Keerthikumar, D. Chisanga, R. Alessandro, C.-S. Ang, P. Askenase, A.O. Batagov, A. Benito-Martin, G. Camussi, A. Clayton, F. Collino, D. Di Vizio, J.M. Falcon-Perez, P. Fonseca, P. Fonseka, S. Fontana, Y.S. Gho, A. Hendrix, E.N.-'t Hoen, N. Iraci, K. Kastaniegaard, T. Kislinger, J. Kowal, I.V. Kurochkin, T. Leonardi, Y. Liang, A. Llorente, T.R. Lunavat, S. Maji, F. Monteleone, A. Øverbye, T. Panaretakis, T. Patel, H. Peinado, S. Pluchino, S. Principe, G. Ronquist, F. Royo, S. Sahoo, C. Spinelli, A. Stensballe, C. Théry, M.J.C. van Herwijnen, M. Wauben, J.L. Welton, K. Zhao, S. Mathivanan, A novel community driven software for functional enrichment analysis of extracellular vesicles data, *J Extracell Vesicles.* 6 (2017) 1321455. <https://doi.org/10.1080/20013078.2017.1321455>.
- [63] D. Szklarczyk, A.L. Gable, D. Lyon, A. Junge, S. Wyder, J. Huerta-Cepas, M. Simonovic, N.T. Doncheva, J.H. Morris, P. Bork, L.J. Jensen, C. von Mering, STRING v11: protein-protein association networks with increased coverage, supporting functional discovery in genome-wide experimental datasets, *Nucleic Acids Res.* 47 (2019) D607–D613. <https://doi.org/10.1093/nar/gky1131>.
- [64] J. Cox, M. Mann, MaxQuant enables high peptide identification rates, individualized p.p.b.-range mass accuracies and proteome-wide protein quantification, *Nat. Biotechnol.* 26 (2008) 1367–1372. <https://doi.org/10.1038/nbt.1511>.
- [65] J. Cox, N. Neuhauser, A. Michalski, R.A. Scheltema, J.V. Olsen, M. Mann, Andromeda: a peptide search engine integrated into the MaxQuant environment, *J. Proteome Res.* 10 (2011) 1794–1805. <https://doi.org/10.1021/pr101065j>.
- [66] M. Ringnér, What is principal component analysis?, *Nat. Biotechnol.* 26 (2008) 303–304. <https://doi.org/10.1038/nbt0308-303>.

Author contributions

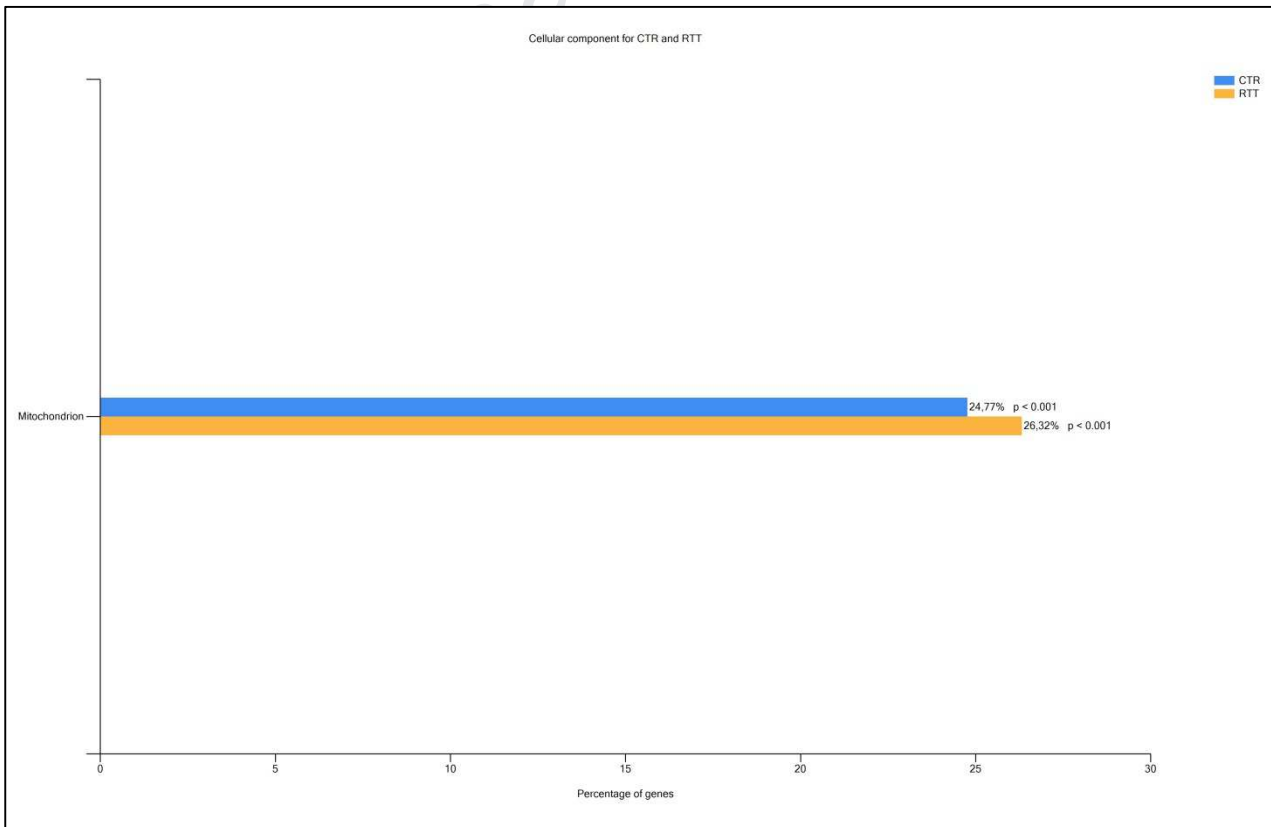
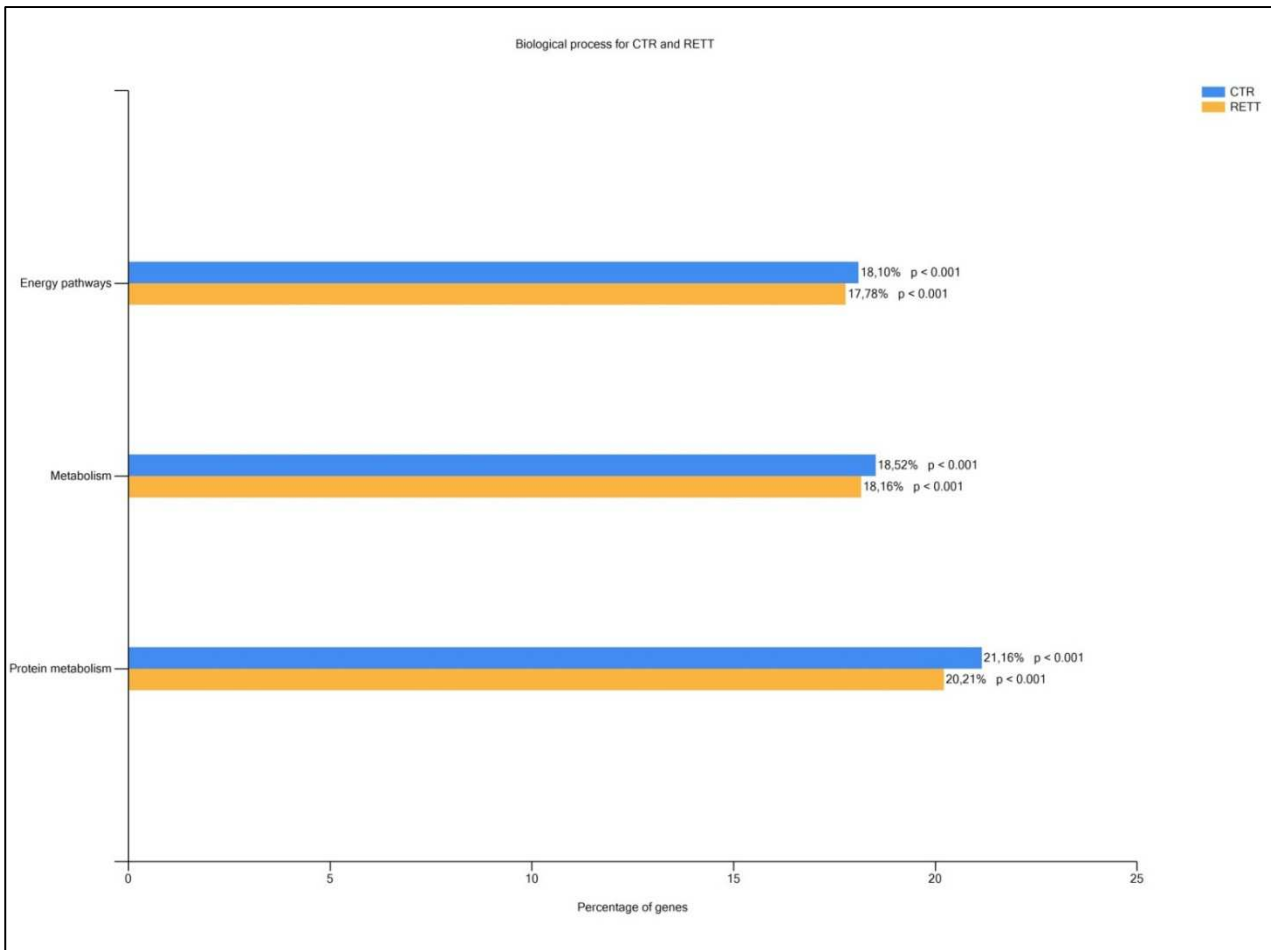
VC performed bioinformatics analysis and analyze data; AP, LT, MR, CC performed experiments; VC, AP, GV wrote the paper; OS, AS, GV edited the paper; JH, LS, CT, GV provided reagents conceptualized experiments and supervised the project.

Journal Pre-proof

Supplementary information



S1. Quality control filtering of mass spectrometry measurements. Protein quantification was performed using MaxQuant label free algorithm (LFQ) with unique and razor peptides for protein quantification. Technical replicates were compared and Spearman rank correlation of LFQ-intensity of the replicates for every sample was calculated. The diagram shows high correlation not only among the technical but also for the biological replicates. Light blue numbers represent the Spearman rank correlation values for each dot-plot. High values (> 0.894) represents a highly reproducible, relative LFQ between replicates.



S2. GO functional annotation comparison. Comparison of RTT common dataset (1154 proteins) and CTR common dataset (1291 proteins) to identify differences (p -value < 0.001) between basal biological processes like “cell growth and/or maintenance” (GO:0016049), “energy pathway” (GO:0006091) and “protein metabolism” (GO:0051246), confirming a general decrease in the number of proteins implicated in the principal functions of RTT cells in comparison to CTR. However, the percentage of proteins involved in the cellular component “mitochondrion” (GO:0005739) resulted to be higher in RTT than in CTR common dataset

Competing Interests

The authors declare no competing interests.

Journal Pre-proof

Highlights

- Proteomic data mining reveals a distinct proteomic profile of RTT fibroblasts
- Several differentially expressed proteins in RTT belong to cell component mitochondrion
- RTT cells show altered expression levels of mitochondrial fusion and mitophagy genes
- Mitophagy is impaired in RTT fibroblasts
- Ultrastructural analysis of RTT cells identify elongated mitochondria with blurry cristae